Aus der Neurologischen Universitätsklinik Tübingen

Abteilung Neurologie mit Schwerpunkt Epileptologie

Characterization of variants in the *KCNQ5* gene associated with genetic generalized epilepsy

Inaugural-Dissertation
zur Erlangung des Doktorgrades
der Medizin

der Medizinischen Fakultät
der Eberhard Karls University
zu Tübingen

vorgelegt von

Yan, Pu

2022

Dekan:	Professor Dr. B. Pichler
1. Berichterstatter:	Professor Dr. H. Lerche
2. Berichterstatter:	Professorin Dr. M. Knipper-Breer
Tag der Disputation:	14.03.2022

CONTENTS

List of Abbreviations

AEDs	Anti-epileptic drugs
AP	Action potential
BBB	Blood-brain-barrier
BFNE	Benign Familial Neonatal Epilepsy
C	Constant term
CAE	Childhood absence epilepsy
CHO	Chinese hamster ovary
CNS	Central nervous system
CaM	Calmodulin
DEEs	Developmental and epileptic encephalopathies
DNA	Deoxyribonucleic acid
E	Excitation
EEG	Electroencephalography
eGFP	Enhanced Green Fluorescent Protein
EGTA	Ethylene glycol-bis(β-aminoethyl ether)-N,N,N′,N′-tetraacetic acid
FCS	Fetal calf serum
FS	Febrile convulsion
GABA	Aminobutyric acid
GEFS+	Generalized epilepsy with febrile seizures plus
GGE	Genetic generalized epilepsy
GLU	Glutamic acid
GOF	Gain-of-function
GSW	Generalized spike-wave
GTCS	Generalized tonic clonic seizure

HGNC	Human Genome Organization (HUGO) Gene Nomenclature Committee
HEPES	4-(2-hydroxyethyl)-1-piperazineethanesulfonic acid
I	Inhibition
ID	Intellectual disability
IGE	Idiopathic generalized epilepsy
ILAE	International League Against Epilepsy
IUPHAR	International Union of Pharmacology
JME	Juvenile myoclonic epilepsy
K	Slope factor
LOF	Loss-of-function
mAchR	Muscarinic acetylcholine receptor
PNS	Peripheral nervous system
$PI(4,5)P_2$	Phosphatidylinositol 4,5-bisphosphate
PLC	Phosphalipase Cβ
RPE	Retinal pigment epithelium
SMEI	Severe myoclonic epilepsy of infancy
TEVC	Two-electrode voltage clamp
TMs	Transmembrane segment
VGCCs	Voltage-gated calcium channels
VGPCs	Voltage-gated potassium channels
VGSCs	Voltage-gated sodium channels
$V_{1/2}$	Half-maximum voltage
WT	Wild type

List of Tables

List of Figures

1 Introduction

1.1 Epilepsy

1.1.1 Definition and classification of epilepsy

Epilepsy is one of the most common chronic disorders of the central nervous system (CNS), and it can affect people of all ages. Epilepsy is defined as a condition of recurrent and unpredictable seizures, characterized by paroxysmal, transient, and stereotyped events and other symptoms, such as changes to sense of smell, touch, hearing or sight, biting of the tongue, and so on (Scheffer *et al.* 2017). These seizures have a variety of underlying causes and hereditary routes; as a result, the clinical manifestations can affect a variety of systems, including the sensory, motor, autonomic, consciousness, mental, memory, and cognitive systems (Fisher *et al.* 2005). The League Against Epilepsy (ILAE) defines abnormal neuronal firing in the cerebrum, thalamocortical system and upper midbrain resulting in abnormal hypersynchronous discharges causing a hyperexcitability of the brain as the primary cause of epileptic seizures (Engel 2001). The ILAE has categorized epileptic seizures into several types to evaluate patients presenting with seizures and to make a clinical diagnosis. This classification is compatible with the ILAE classification from 1989 and its latest revision from 2017 (Scheffer *et al.* 2017), including generalized seizures, focal seizures, and seizures of unknown origin, each of which is subdivided into motor and nonmotor seizures (Fig. 1) (Fisher *et al.* 2017b; Stafstrom and Carmant 2015). In addition, there is also a new seizure group described as combined generalized and focal seizures (Scheffer *et al.* 2017).

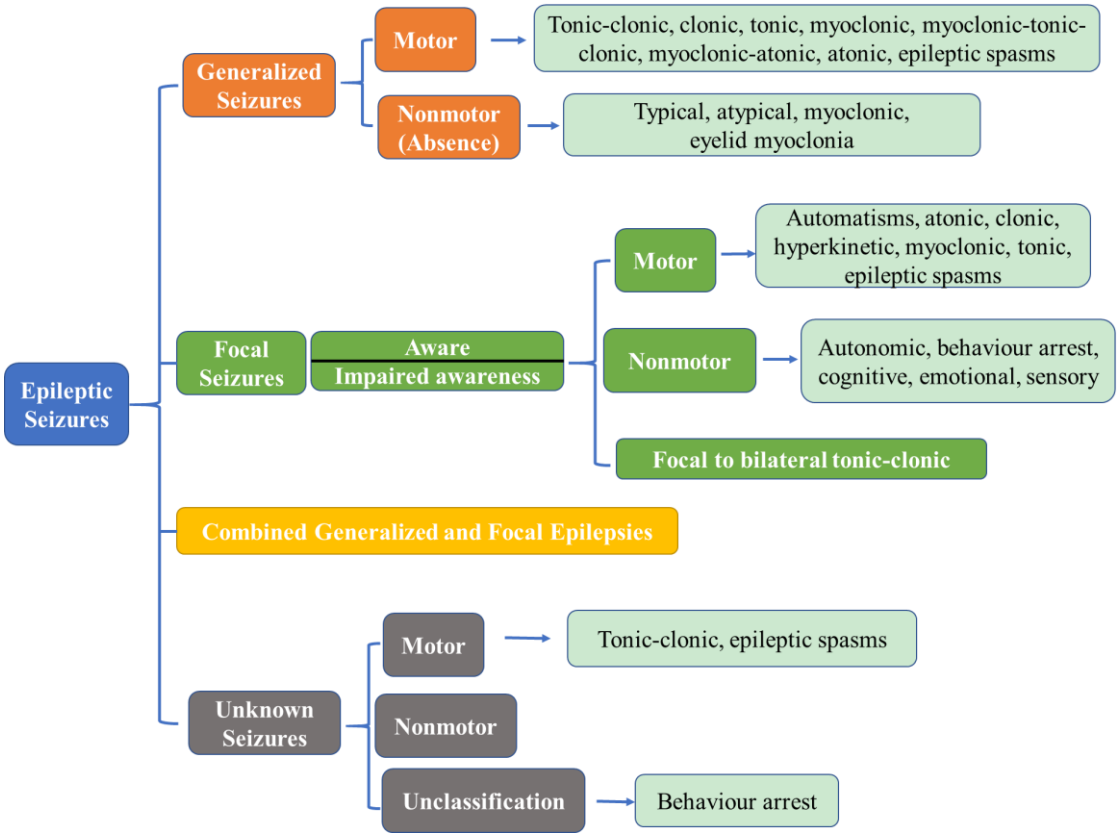

Fig. 1 The 2017 classification of epileptic seizures by the ILAE. There are several epileptic seizures, namely generalized, focal, combined generalized and focal, and seizures of unknown origin. Each type of seizure is subsequently subdivided into motor and nonmotor onset. This figure was modified from Scheffer *et al*. (2017); Fisher *et al*. (2017a); Fisher *et al*. (2017b).

In generalized seizures, the presence of bilateral generalized epileptic discharges is regarded with the utmost priority, and the focus is such discharges occur on both hemispheres at the same time (Scheffer *et al.* 2017). Notably, generalized seizures should be diagnosed in accordance with additional clinical findings, such as relevant family histories and findings from electroencephalography (EEG) recordings (mainly generalized spike wave (GSW) activity) (Koutroumanidis *et al.* 2005; Scheffer *et al.* 2017). Specifically, generalized seizures are subgrouped by their symptoms at onset as those with motor (clonic, atonic, tonic, tonic-clonic, myoclonic, myoclonic-tonic-clonic, and myoclonic-atonic) or nonmotor (typical/atypical absence, myoclonaic, and eyelid myoclonia) onset (Fisher *et al.* 2017b). Focal seizures include unifocal and multifocal onset, both of which are confined within one brain hemisphere. In other words, the clinical manifestations of focal epileptic seizures therefore may vary depending on where the focus is located within the cortex or deeper brain structures. For instance, when the seizure focus is located in the precentral gyrus, the patient presents rhythmic clonic or tonic motor activity; in contrast, sensory symptoms, such as paresthesia, occur when the focal seizure arises from the postcentral gyrus (Stafstrom and Carmant 2015). Therefore, focal seizures should also be diagnosed based on clinical conditions and supported by EEG findings (namely, focal epileptiform discharges), which is a valid method for determining the localization of focal seizures (Foldvary *et al.* 2001). They are also divided into motor and nonmotor seizures, with the added component of the patient's awareness level (Fisher *et al.* 2017b). Focal motor onset includes automatisms, atonia, clonus, hyperkinesia, myoclonus and tonics, whereas focal nonmotor onset incorporates autonomic behavioral arrest, as well as cognitive, emotional, and sensory onset.

Individuals who had both focal and generalized seizures were considered a new group of epileptic seizures, and the new term in use is combined generalized and focal seizures

(Scheffer *et al.* 2017). Additional clinical manifestations (relevant family histories) and findings from EEG recordings (both focal epileptiform discharges and generalized spike-wave, but for the diagnosis epileptiform activity is not required), should be utilized in order to properly diagnose this type of seizure (Fisher *et al.* 2017a; Scheffer *et al.* 2017). Dravet syndrome and Lennox-Gastaut syndrome are both well-known instances of conditions that have both generalized and focal seizures (Scheffer *et al.* 2017).

Epileptic spasms suggest epilepsy, but it can be difficult for clinicians to distinguish a diagnosed case of epileptic seizure as being focal or generalized. Typically, sudden flexion, extension, or a combination of both in proximal and truncal muscles are characteristic of epileptic spasms, and such symptoms often appear in cluster (Blume *et al.* 2001; Stafstrom and Carmant 2015). As a result, the onset of epileptic spasms is often more protracted than a myoclonic seizure, but not as prolonged as a tonic seizure.

1.1.2 Etiologies of epilepsy

A great number of recent researches on epilepsy have revealed that its pathogenic mechanisms are quite intricate and complex. Epilepsy is typically attributed to an imbalance in the excitation (E) and inhibition (I) of CNS (Stafstrom and Carmant 2015). Imbalanced E/I in the CNS can result from various abnormalities at many different levels. Function of excitatory synapsis develops earlier than function of inhibitory synapsis in a normally developing brain. While early in development, the neurotransmitter γ-aminobutyric acid (GABA) induces excitation, it later turns into one of the most important inhibitory neurotransmitters (Ben-Ari 2002; Pitkänen *et al.* 2015). Such findings support the hypothesis that the normal developing brain is vulnerable to the occurrence of seizures. In the latest classification of epilepsies in 2017, Scheffer and her colleagues differentiated six etiologies of epilepsy: structural, metabolic, immune, genetic, infectious, and

unknown (Scheffer *et al.* 2017). Alterations in brain structure can induce epileptic seizures. These alterations may have any number of different etiologies, including stroke, tumors, trauma, metabolic or neurodegenerative disorders. Determining the appropriate feasible etiology at the time of an epileptic seizure could facilitate the diagnosis and treatment of epilepsy patients. For example, a focal cortical dysplasia or a malignant tumor could induced a wide range of symptomatic seizures (Kirschstein and Köhling 2016; Adhikari *et al.* 2021), to find and treat the primary disease is the most important thing to reduce epileptic seizures. Furthermore, animal and human models suggest that strong immune responses can result in damage to the blood-brain barrier (BBB), induced by several factors, giving rise to epileptic seizures (Vezzani *et al.* 2011; Dubé *et al.* 2005; Kulkarni and Dhir 2009; Riazi *et al.* 2010). However, greater than 30% of epileptic seizures have a genetic etiology unrelated to any structural brain abnormality (Weber *et al.* 2017; Weber and Lerche 2013). Epilepsy induced by genetic etiology are named as genetic epilepsy, including genetic generalized epilepsy (GGE), developmental epileptic encephalopathies (DEEs) and genetic focal epilepsy (Weber *et al.* 2017).

Since the discovery of the first variant in connection with epilepsy, a gene encoding the cholinergic nicotinic α4-subunit (*CHRNA4*) which was identified to correlate to the autosomal dominant nocturnal frontal lobe epilepsy (Steinlein *et al.* 1994), researchers have described many new epilepsy-related variants and genes. These variants mainly occur in genes coding for ligand- and voltage-gated ion channels, as well as auxiliary subunits. For examples, Dravet syndrome, which was identified as one of the first genetic epilepsy syndromes and known as severe myoclonic epilepsy of infancy (SMEI), was found to be caused by the variants of the *SCN1A* gene and abnormality of the *SCN1A*-coded voltage-gated sodium channel (VGSC) $Na_v1.1$ (Claes *et al.* 2001). Furthermore, *KCNQ2* and *KCNQ3* variants, which encode voltage-gated potassium channels (VGPCs),

have been identified in benign familial neonatal epilepsy (BFNE) (Biervert *et al.* 1998). Additionally, variants in *GABRA1-3* gene (Maljevic *et al.* 2019), *GABRG2* gene (Milanovska *et al.* 2021) and *KCNQ5* gene (Krüger *et al.* 2021) have been reported to be associated with GGE.

1.2 Genetic generalized epilepsy (GGE)

Genetic generalized epilepsy (GGE) that is trigged by known and unknown genetic causes (previously known as idiopathic generalized epilepsy (IGE)) is described as a type of generalized epilepsy without any structural brain abnormalities (Berkovic and Scheffer 2001; Scheffer *et al.* 2017). The characteristic EEG of GGE shows epilepsy discharges at 2.5-5 Hz epileptic discharges on a normal background (Duncan 1997). One-third of GGE patients have a family history of epilepsy, including childhood and juvenile absence epilepsy and other syndromes (Nolan and Fink 2018). GGE mainly encompasses the four most common syndromes: childhood absence epilepsy (CAE), juvenile absence epilepsy (JAE), juvenile myoclonic epilepsy (JME) and epilepsy with generalized tonic-clonic seizures alone (EGTCS) (Scheffer *et al.* 2017).

1.2.1 Childhood absence epilepsy (CAE) and juvenile absence epilepsy (JAE)

CAE and JAE can be distinguished by several criteria. CAE is the most common condition and generally occurs in children aged four to ten, whereas JAE is found in children over ten. CAE ictal EEGs generally have GSW with a 3 Hz frequency and high amplitude of 200-300 μV, with a maximum in the frontal midline (Moeller *et al.* 2017). The GSW seen in JAE has a slightly higher frequency, at 3.5-4 Hz (Moeller *et al.* 2017). CAE patients have several hundred absence seizures per day (Sadleir *et al.* 2006), which last between 1-45 s (Sadleir *et al.* 2006), while patients experiencing JAE are subjected

to less frequent absence seizures, even fewer than one per day. JAE patients can also experience generalized tonic-clonic seizures (GTCSs) and sporadic myoclonic seizures (Janz 1997). Several variants have been associated with GGE, such as those in the $GABA_A$ receptor gene *GABRA1-3* (Baulac *et al.* 2001; Maljevic *et al.* 2019; May *et al.* 2018; Wallace *et al.* 2001; Nolan and Fink 2018).

1.2.2 Juvenile myoclonic epilepsy (JME)

JME, which is characterized by seizures with bilateral jerks, usually arises around puberty and was first described by Janz (Janz 1985). Because these jerks occur predominantly in the arms or legs, patients may fall suddenly, usually without loss of consciousness (Nolan and Fink 2018). The interictal EEG of JME shows generalized spike and polyspike waves from 3 to 6 Hz arising from a normal background. Approximately half of these patients have a family history of epilepsy (Guerrini *et al.* 2019). Previous studies had reported associations with autosomal dominant variants in $GABA_A$ receptor genes, such as *GABRA1* (Cossette *et al.* 2002; Maljevic *et al.* 2019; May *et al.* 2018).

1.2.3 Epilepsy with generalized tonic-clonic seizures alone (EGTCS)

EGTCS is a syndrome with generalized tonic-clonic seizures (GTCS), which was formerly called epilepsy with grand mal (generalized tonic-clonic) seizures. EGTCS usually starts in adolescence, and seizures can happen at any time of the day, although they are often clustered in the first 2 hours after awakening (Scheffer *et al.* 2017). Interictal EEG of EGTCS patients shows generalized fast spike and polyspike wave discharges (3-5 Hz) with a normal background, which is similar to those of JME (Scheffer *et al.* 2017).

Apart from several variants in $GABA_A$ receptor genes, GGEs in general were reported to be associated with microdeletion on chromosome 15, which includes the *CHRNA7* gene, first described by Helbig *et al.* (2009). Although variants in $GABA_A$ receptor genes or microdeletions on chromosome 15 associated with GGEs have been reported (Hirose 2014; Helbig *et al.* 2009), to date, no gene specific to EGTCS has been identified.

1.3 Ion channel alterations associated with epilepsy

Ion channels, which are pore-forming transmembrane proteins, lay the physical foundation of cellular electric activity. The selectively let ions go through the cell membrane through their pores following electrochemical gradients, making them a critical participant in cell excitability (de Lera Ruiz and Kraus 2015; Hinard *et al.* 2016; Hille 1978). Variants in ion channel genes can result in many disorders, collectively known as channelopathies, such as epilepsy, nondystrophic myotonias, periodic paralysis, migraine, and episodic ataxia (Kim 2014). Ligand- and voltage-gated channels are both the most abundant and the most pivotal channels in the membrane (Wetsel 2011; Hinard *et al.* 2016; Nilius and Honoré 2012). Specifically, voltage-gated ion channels can adopt one of the three general conformational states in response to membrane potential, which are marked as open, closed, or inactivated states (Fig. 2).

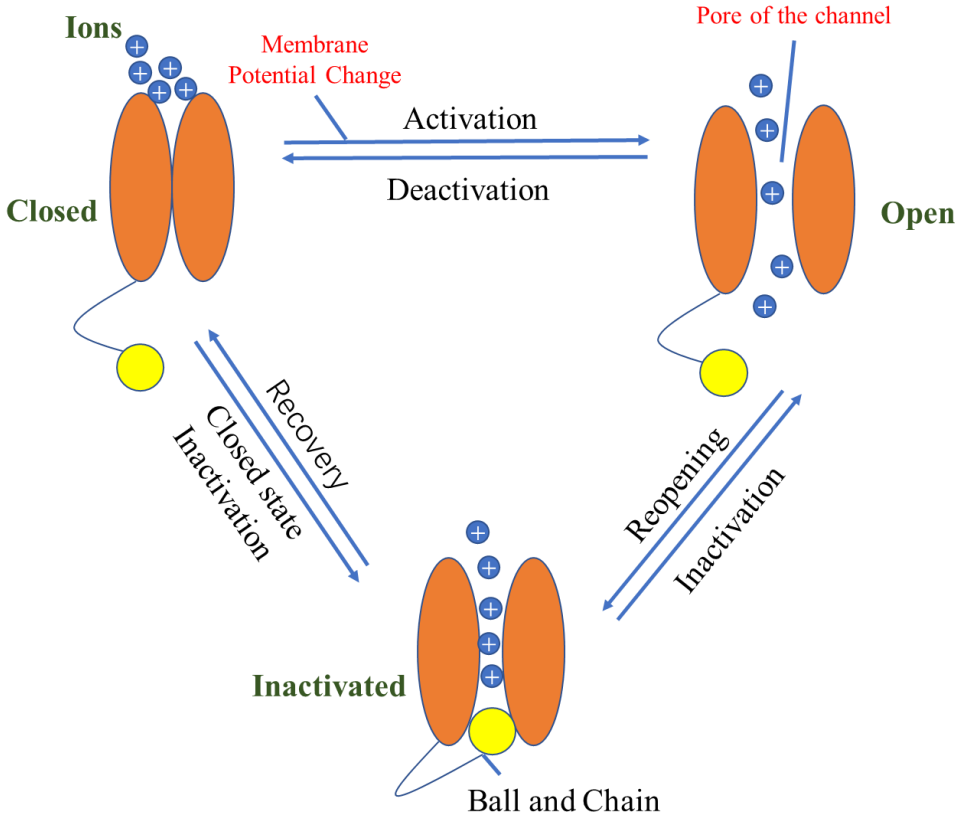

Fig. 2 Three conformational states of voltage-gated ion channels. The open, closed, and inactivated states are depicted in a figure modified from Hinard *et al.* (2016).

Structural abnormalities or dysfunction of voltage-gated ion channels can affect the electrophysiological properties of the neurons. Voltage-gated channels for calcium, sodium, and potassium ions, which are abbreviated as VGCCs, VGSCs, VGPCs, respectively, are crucial to maintaining the balance of E/I in neurons. As is mentioned in section 1.1.2 above, an imbalance between E and I in brain networks can lead to excessive and hypersynchronous discharges, which can induce epilepsy. In 1952, Hodgkin and Huxley described the voltage-gated sodium current based on their analysis of the squid giant axon (Hodgkin and Huxley 1952). VGSCs have since been discovered to include one α-subunit and either one or two β-subunits (de Lera Ruiz and Kraus 2015; Heine *et al.* 2016). until now, nine subtypes of the human Na_V channel subtypes (Na_V 1.1 to Na_V 1.9) have been identified (de Lera Ruiz and Kraus 2015). Among these Na_V channels subtypes, the majority of epilepsy causes have been found to associate with Nav1.1 (*SCN1A*), Nav1.2 (*SCN2A*), and Nav1.6 (*SCN8A*) (de Lera Ruiz and Kraus 2015). For example, *SCN1A* variants are correlated to febrile seizures (FS), generalized epilepsy with febrile seizures plus (GEFS+), Doose syndrome, and Dravet syndrome (Scheffer and Nabbout 2019).

Meanwhile, VGCCs variants are also important to maintain the E/I balance in brain neurons. The Ca^{2+} ion channel was first distinguished in muscle cells (Fatt and Katz 1953). In the CNS, most calcium channels are VGCCs, and they are associated with epilepsy, migraine, and ataxia (Rajakulendran and Hanna 2016). The function of VGCCs is to depolarize a cell through their activation. The paroxysmal depolarizing shift, the synchronous discharge of neurons, and the formation of inhibitory postsynaptic potential are affected by fast or slow influx of Ca^{2+} ions. For example, variants in *CACNA1A* have been reported to result in absence epilepsy, although further research suggests that these variants can also be identified in episodic ataxia type 2, familial hemiplegic migraine, and

spinocerebellar ataxia type 6 (Kors *et al.* 2004).

1.3.1 K^+ channel alterations associated with epilepsy

As one of the most crucial and widespread ion channels in the cell membrane, K^+ channels are distributed in the skeletal, cardiovascular, and nervous systems as a critical participant of cell membrane excitability. Based on the transmembrane segments (TMs), K^+ channels can be categorized as 2-TMs potassium channels (inward-rectifier potassium channels, K_{ir}), 4-TMs potassium channels (four transmembrane segment-2 pores, K_{2P}), 6-TMs potassium channels (VGPCs, K_V), Ca^{2+}-activated potassium channels (SK_{Ca}) and 7-TMs potassium channels (Fig. 3) (González *et al.* 2012; Gutman *et al.* 2005; Köhling and Wolfart 2016; Kuang *et al.* 2015).

A 2-TMs Inward rectifiers (K_{ir})

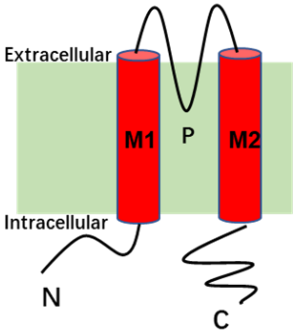

B 4-TMs-2 Pores (K_{2P})

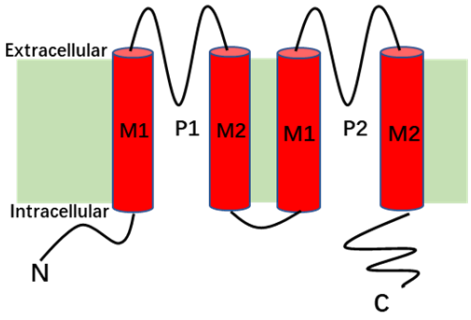

C 6-TMs Voltage-gated K^+ Channel (K_V)

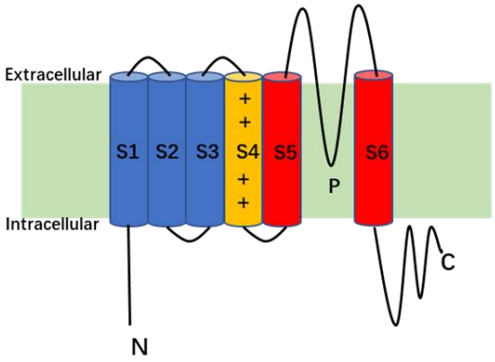

D 6-TMs Calcium-activated K^+ channels (SK_{Ca})

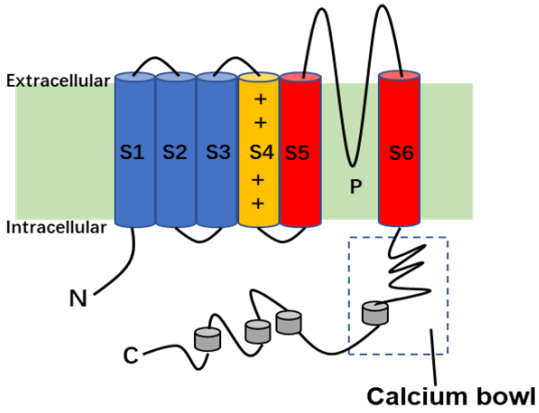

E 7-TMs the Slo family

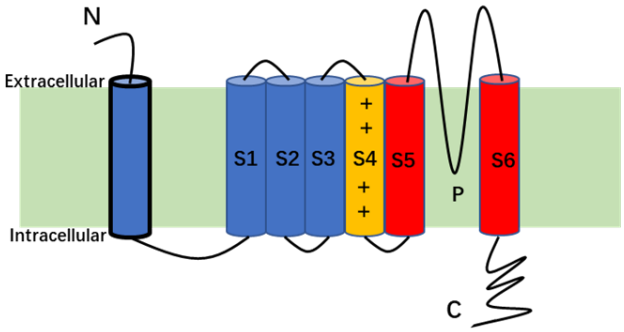

Fig. 3 Classification of K^+ channels. (A) 2 TMs, the inward-rectifier K^+ channels (K_{ir}); **(B)** 4 TMs, four transmembrane segments-2 pores (K_{2P}); **(C)** 6 TMs, voltage-gated potassium channel (K_V); **(D)** 6 TMs, calcium-activated K+ channels (SK_{Ca}); **(E)** 7 TMs, the Slo family (González *et al.* 2012; Gutman *et al.* 2005; Köhling and Wolfart 2016; Kuang *et al.* 2015).

VGPCs, which have attracted widespread attention from researchers, are the largest group of potassium channels. By maintaining a slow and continuous outgoing potassium current, VGPCs are vital controllers of the cellular resting potential. Moreover, the efflux of K^+ ions is the dominant factor when the neuronal action potential is descending, and such efflux to the extracellular fluid is made possible by the opening VGPCs. Therefore, VGPCs can mediate the repolarization and subsequent hyperpolarization of neurons (Fig. 4) (Kim and Nimigean 2016).

A

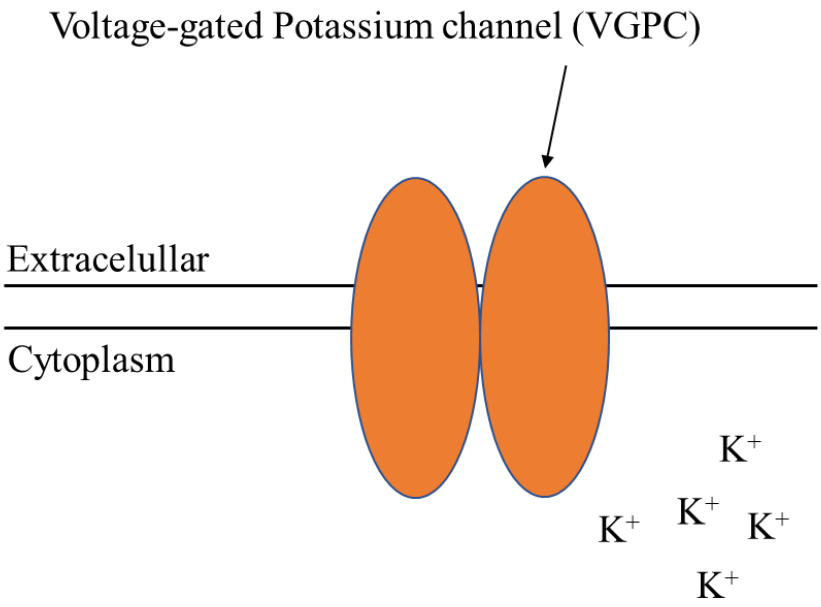
Voltage-gated Potassium channel (VGPC)
Extracelullar
Cytoplasm
K+
K+
K+
K+
K+

B

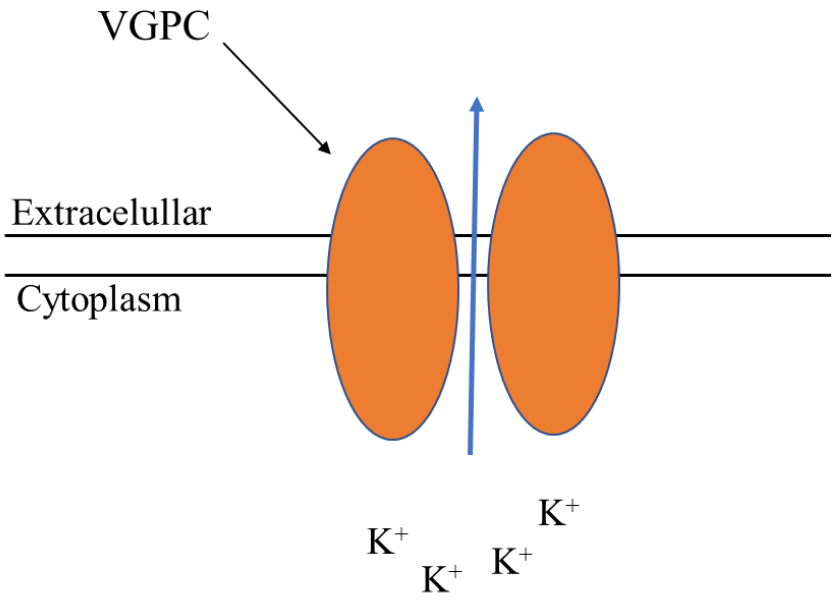
VGPC
Extracelullar
Cytoplasm
K+
K+
K+
K+

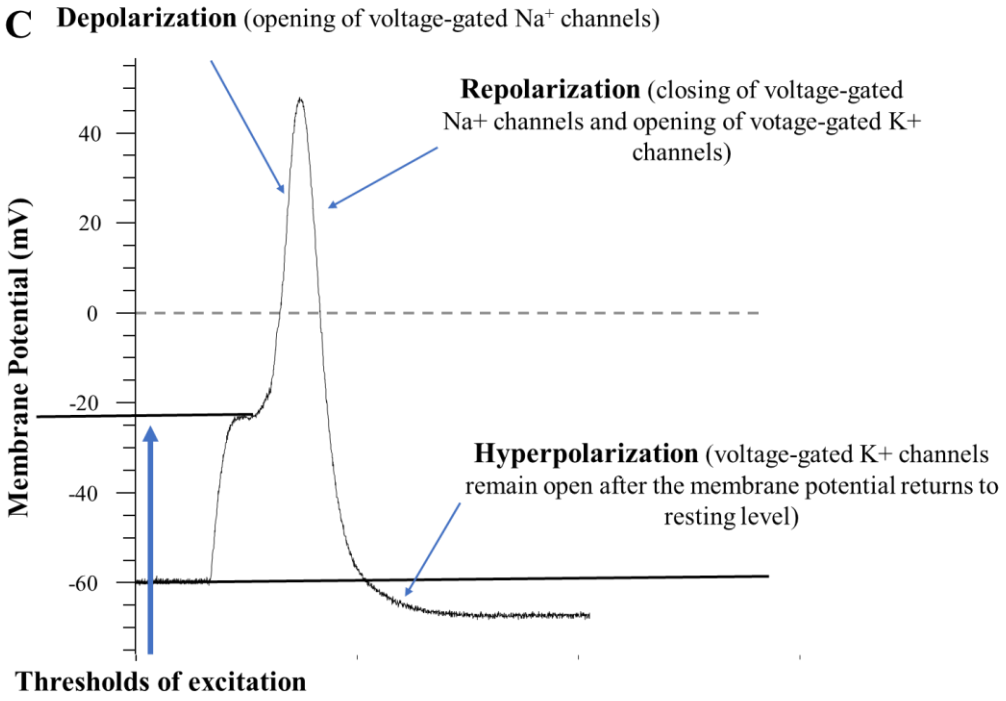

Fig. 4 Two states of VGPCs and their influence on the AP. (A) The closed state showing an absence of K^+ efflux. **(B)** The open state resulting in an efflux of K^+ ions. **(C)** Action potential (AP). The rising phase corresponds to membrane depolarization and VGSC openness. At the peak of the curve, the VGSCs begin to close, and the VGPCs start to open, suggesting membrane repolarization. After the membrane potential returns to the resting potential, the VGPCs remain open, resulting in membrane hyperpolarization.

The structure of VGPCs consists of four α-subunits and sometimes additional auxiliary subunits (β-subunits), and the α-subunits are the focus of the current study. VGPCs are 6-TMs potassium channels, which are characterized by 6 TMs (S1-S6) in each α-subunit. Particularly, S1-S4 subunits constitute the voltage-sensing domains in which S4 is the voltage-sensor (Shah and Aizenman 2014). The S5-Pore-S6 (S5-P-S6) segment makes up the pore domain, which is a selective potassium filter (Fig. 5A) (Shah and Aizenman 2014). The crystal structure of VGPC is shown in figure 5B, which is from Long *et al.* (2005). Approximately 40 genes of 12 families, K_V1-K_V12, encode the K_V α-subunits in mammals. The genes are categorized based on their structures, properties, and pharmacological profiles (Table 1) (Chen *et al.* 2017; Gutman *et al.* 2005; Köhling and Wolfart 2016; Meneses *et al.* 2016).

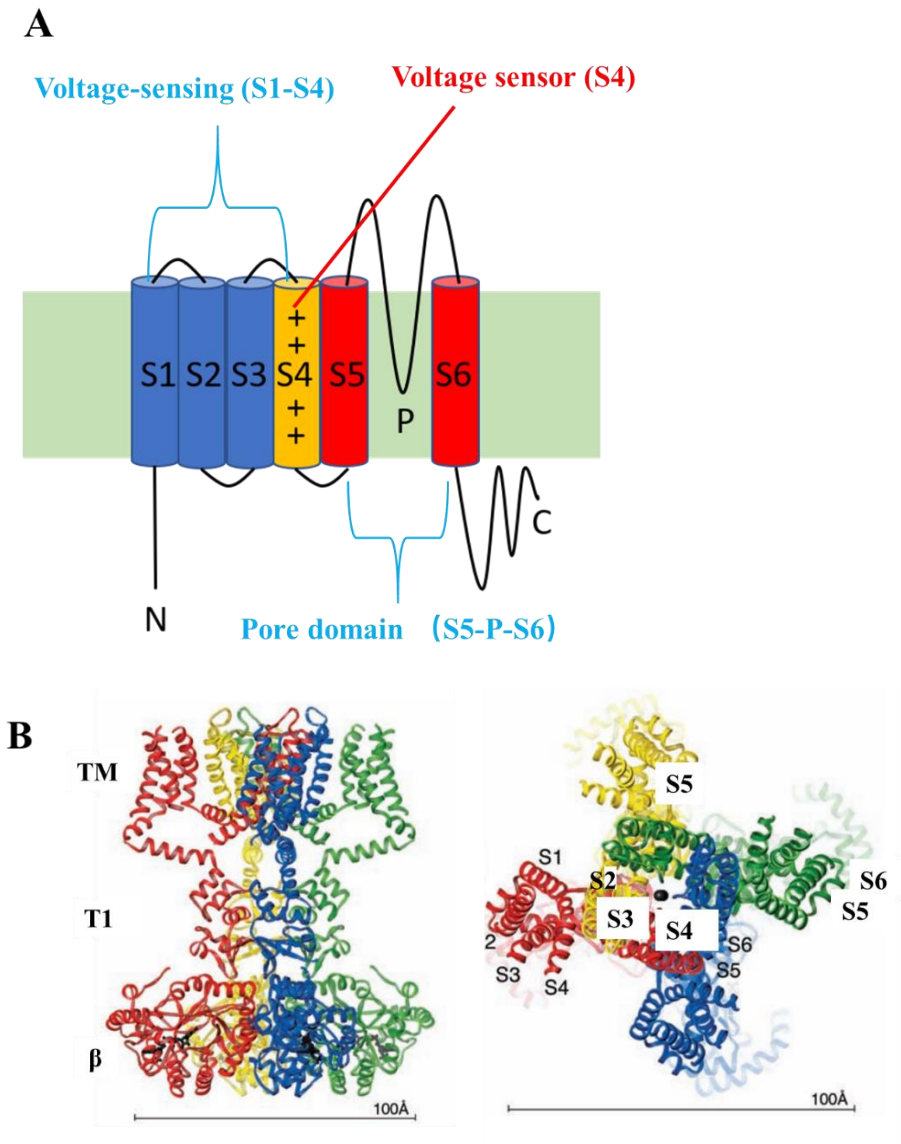

Fig. 5 Structure of α-subunits of the Kv channel. Each channel may be composed of different α-subunits, and they are fundamentally heteromers (Shah and Aizenman 2014). **(A)** shows that the S1-S4 segments constitute the voltage-sensor domains (blue and yellow), and the S4 segments (yellow) are the voltage sensors. In addition, the S5-P-S6 segment forms the pore region (red). **(B)** represents $K_V1.2$ -β_2 subunit complex crystal structure. The upper figure depicts a side stereoview of a ribbon depiction, in which the voltage sensor, T1 domain, and pore domain are shown as four colored

subunits. The lower figure shows a stereoview of a ribbon depiction, seen from the extracellular side of the pore domain, whose structure was been by electron microscopy (Long *et al.* 2005). TM = transmembrane segment.

Table 1 The VGPC subunits named by the International Union of Pharmacology (IUPHAR) and the corresponding gene names defined by the HUGO Gene Nomenclature Committee (HGNC)

IUPHAR		HGNC	Chromosome loci
K_V1	$K_V1.1$	*KCNA1*	12p13
	$K_V1.2$	*KCNA2*	1p13
	$K_V1.3$	*KCNA3*	1p21
	$K_V1.4$	*KCNA4*	11p14
	$K_V1.5$	*KCNA5*	12p13
	$K_V1.6$	*KCNA6*	12p13
	$K_V1.7$	*KCNA7*	19q13
	$K_V1.8$	*KCNA1*	1p13
K_V2	$K_V2.1$	*KCNB1*	20q13
	$K_V2.2$	*KCNB2*	8q13
K_V3	$K_V3.1$	*KCNC1*	11p14
	$K_V3.2$	*KCNC2*	19q13
	$K_V3.3$	*KCNC3*	19q13
	$K_V3.4$	*KCNC4*	1p21
K_V4	$K_V4.1$	*KCND1*	Xp11
	$K_V4.2$	*KCND2*	7q31
	$K_V4.3$	*KCND3*	1p13
K_V5	$K_V5.1$	*KCNF1*	2p25

K_V6	$K_V6.1$	*KCNG1*	20q13
	$K_V6.2$	*KCNG2*	18q22
	$K_V6.3$	*KCNG3*	2p21
	$K_V6.4$	*KCNG4*	16q24
K_V7	$K_V7.1$	*KCNQ1*	11p15
	$K_V7.2$	*KCNQ2*	20q13
	$K_V7.3$	*KCNQ3*	8q24
	$K_V7.4$	*KCNQ4*	1p34
	$K_V7.5$	*KCNQ5*	6q14
K_V8	$K_V8.1$	*KCNV1*	8q22
	$K_V8.2$	*KCNV2*	9p24
K_V9	$K_V9.1$	*KCNS1*	20q12
	$K_V9.2$	*KCNS2*	8q22
	$K_V9.3$	*KCNS3*	2p24
K_V10	$K_V10.1$	*KCNH1*	1q32
	$K_V10.2$	*KCNH5*	14q23
K_V11	$K_V11.1$	*KCNH2*	7q35
	$K_V11.2$	*KCNH6*	17q23
	$K_V11.3$	*KCNH7*	2q24
K_V12	$K_V12.1$	*KCNH8*	3p24
	$K_V12.2$	*KCNH3*	12q13
	$K_V12.3$	*KCNH4*	17q21

1.3.1.1 The VGPC K_V7 family and the $K_V7.5$ channel

K_V7 channels were first identified by Brown and Adams in 1980 (Brown and Adams 1980). While investigating the activation of muscarinic acetylcholine receptors (mAchRs) on the superior cervical ganglia of *Rana catesbeiana* (Shaw), they found that the activation of mAchRs could inhibit K_V7 currents (Brown and Adams 1980). K_V7 channels are named muscarinic channels (M channels) due to their inhibition by muscarinic agonists and generate a voltage-dependent, slowly activating, and non-inactivating

potassium current (Brown and Adams 1980; Wuttke *et al.* 2005; Lerche *et al.* 2000; Xiong *et al.* 2007; Dorange and Swahn 2011). Previously, kinetics of the M current could be down-regulated by metabotropic G-protein-coupled receptors, which induce hydrolysis and depletion of phosphatidylinositol 4,5-bisphosphate (PIP_2) from the membrane by phospholipase Cβ (PLC) (Suh and Hille 2007; Zhang *et al.* 2003), regulating the membrane potential at threshold voltages and thus affecting neuronal firing and excitability (Brown and Adams 1980; Brown and Passmore 2009).

The K_V7 channel subunits of VGPCs are encoded by the *KCNQ* gene family. Under most conditions, they are predominantly co-expressed with the small β-subunits encoded by the *KCNE* gene family (Robbins 2001). K_V7 channels have a similar 6 TMs structure as other K_V channels. Five subtypes of K_V7 channels are $K_V7.1$, $K_V7.2$, $K_V7.3$, $K_V7.4$ and $K_V7.5$, which are encoded by *KCNQ1, KCNQ2, KCNQ3, KCNQ4*, and *KCNQ5*, respectively (Robbins 2001). The different α-subunits of K_V7 channels have distinct functions. *KCNQ1* is found in cardiac muscle and the cochlea (Wang *et al.* 1996), and variants in *KCNQ1* are associated with cardiac arrhythmia or deafness (Abbott and Goldstein 2002; Wang *et al.* 1996). Meanwhile, *KCNQ2* and *KCNQ*3 are mostly expressed in the peripheral and brain nerves (Biervert *et al.* 1998). Previously, variants in the $K_V7.2$ and $K_V7.3$ channels are associated with benign familial neonatal seizures (BFNS) and developmental and epileptic encephalopathies (DEEs) (Brown 2008; Maljevic *et al.* 2010). Moreover, many previous publications have further revealed that the majority of *KCNQ2* mutations and some *KCNQ3* mutations can affect the M current through loss-of-function (LOF) or gain-of-function (GOF), leading to a wide range of epilepsy types in humans (Castaldo *et al.* 2002; Füll *et al.* 2013; Hunter *et al.* 2006; Orhan *et al.* 2014; Miceli *et al.* 2015). *KCNQ4*, which plays a critical role in the auditory system, is found in sensory outer hair cells, and its dysfunction causes non-syndromic dominant

deafness (Kubisch *et al.* 1999).

K_V7.5 channels, which are encoded by the *KCNQ5* (potassium voltage-gated channel KQT-like subfamily, member 5) gene on chromosome 6q13 (Schroeder *et al.* 2000), are present in the CNS, skeletal muscles and blood vessels (Schroeder *et al.* 2000; Brueggemann *et al.* 2007; Lehman *et al.* 2017; Lerche *et al.* 2000). *KCNQ5* poses similar impacts on M currents compared to other K_V7 channels (Zhang *et al.* 2011). Originally, K_V7.5 channels were not shown to have a connection with disease, but the *KCNQ5* gene was recently suggested to be involved in diseases such as high myopia (Liao *et al.* 2017). In 2017, Lehman and his colleagues identified four *de novo KCNQ5* variants (p.Ser448Ile, p.Leu341Ile, p.Val145Gly, and p.Pro369Arg) in four patients with intellectual disability (ID) or DEE (Lehman *et al.* 2017), and their effects were examined by the two-electrode voltage clamp (TEVC) approach. The results showed that the first three variants could cause a LOF, while p.Pro369Arg produced a GOF, suggesting their roles in affected the gating properties of the M current, which may explain why they can lead to ID or DEE (Lehman *et al.* 2017).

1.4 Aim

In 2017, variants in the *KCNQ5* gene were first identified in patients with developmental and epileptic encephalopathy (DEE). This was the first time that *KCNQ5* was reported as an epilepsy-related gene. Other members from the working group in which I was involved in the laboratory of Holger Lerche detected two variants p.Arg359Cys (R359C) and p.Val170Ile (V170I) as the first variants identified in patients with GGE. The objective of my research was to use the whole-cell patch-clamp technique in mammalian cells (Chinese hamster ovary (CHO) cells) transfected with wild type (WT) and/or mutant *KCNQ5* cDNA to investigate the characteristics of these two novel *KCNQ5* variants.

2 Materials and methods

2.1 Mutagenesis

Two inherited *KCNQ5* variants were identified in two GGE families by my colleagues. Then, to detect transfected cells easily under a fluorescence microscope, using molecular cloning methods, my colleague inserted *KCNQ5* WT or one of *KCNQ5* variants (c.508G > A (p.Val170Ile, V170I) or c.1075C > T (p.Arg359Cys, R359C)) into the pcDNA3.1-P2A-eGFP plasmid containing human *KCNQ5* WT cDNA (8938 bp). When exposed to blue light within a certain ultraviolet range, the eGFP expresses bright green fluorescence, making transfected cells visible. The P2A cleavage site ensures that the eGFP is cleaved off of the subunit after transcription.

2.2 DNA purification

Plasmid DNA was purified according to the Genopure Plasmid Maxiprep Kit (Roche) protocol. The concentration of the purified plasmid DNA concentration and the ration of A260/280 were measured by a spectrophotometer (Nano Drop®, Biotechnologie GmbH, USA).

2.3 CHO cell cultures

CHO cells, which have been widely applied in many fields in both industry and science, were first isolated from the ovary of an adult female Chinese hamster in 1958 (Tjio and Puck 1958). Because CHO cells contain a small number of intrinsic potassium channels, numerous recent reports have used them to characterize variants in the *KCNQ2/KCNQ3*

genes variants. Therefore, in this study, CHO cells were thus used to functionally characterize the effects of *KCNQ5* variants.

To split the cultured CHO cells, they were first washed once with PBS. Subsequently, 1 mL of trypsin was added to the cells for approximately one min to sufficiently detach the adherent cells. Afterwards, 10 mL of Ham's F12 medium + 2 mM glutamine +10% fetal calf serum (FCS) were added to dissociate the cells and inactivate the trypsin. Cell density was measured using a 1×1 mm hemocytometer and diluted to approximately 1,000,000 cells/mL and seeded in a new T-75 flask with new media, was the same as those used to dissociate the cells. Cells were incubated at 37℃ with 5% CO_2, and the medium was changed every 72 h.

2.4 Transfection of CHO cells

As one of the most common means to introduce foreign nucleic acids into cells, transfection is also an important tool to study the functions of genes or proteins. In this study, the cationic lipid method is applied because it is more effective and sensitive in cells and tissue slices when there is no limitation from the packaging of foreign DNA (Kim and Eberwine 2010).

Approximately 18-24 h before the transfection, CHO cells were seeded into several 35 mm Petri dishes with F12 medium at an approximate concentration of ~700,000 cell/dish. Before use, the TransIT-LT1 reagent was warmed up from 4℃ to room temperature, followed by gentle vertexing. Then, Opti-MEM reduced-Serum Medium was added to a sterile tube at an amount of 250 µL per well, and 7.5 µL of TransIT-LT1 reagent was added into the tube afterward. The two components were then mixed gently followed by incubation for a 5 min at room temperature. Subsequently, 1 µg of gently mixed *KCNQ5*

WT and/or mutant DNA was added, followed by an additional incubation at room temperature for 20 min. Then, the mixed solutions were then added in drops to the CHO cells. The cells were cultured for 24 h before recording.

2.5 Electrophysiological techniques

In the 19th century, the study of electrophysiological technology by Aloisio Galvani started to be applied to a nerve. In the 20th century, Alan Hodgkin and Andrew Huxley applied a voltage clamp to determine the role of ion channels in nerves (Hodgkin and Huxley 1952). The application of electrophysiological techniques helps researchers to understand the function of neurons from single-channel properties to the connection among the whole nervous system. Because electrophysiological methods are objective, sensitive, and reproducible, they have become a major tool in biophysical research, specifically in the study of neuronal functions (Hodgkin and Huxley 1952).

2.5.1 Introduction to patch-clamp recordings

As the electrophysiological technologies continue to advance, the patch-clamp technique has been developed to measure the capability of single ion channel conductance with microelectrodes by Erwin Neher and Bert Sakmann, the winners of the Nobel Prize for Physiology or Medicine in 1991. The patch-clamp techniques involve four configurations: cell-attached, which are whole-cell, outside-out and inside-out (Fig. 6).

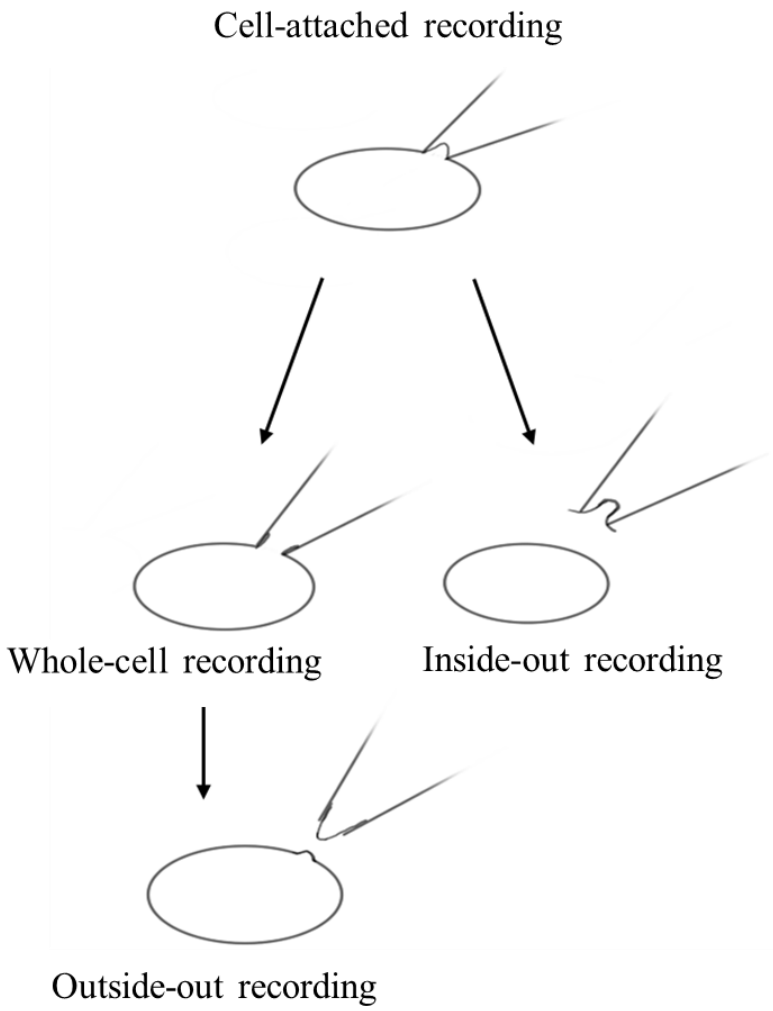

Fig. 6 Four configurations of the patch-clamp technique. Cell-attached, whole-cell, outside-out and inside-out recordings.

Specifically, whole-cell recording is the most commonly used configuration of the patch-clamp technique. When applying whole-cell recording, the cell membrane must be broken with strong suction. Then, the interior of the glass pipette is connected to the cell cytoplasm, which allowing low-resistance electrical access and enabling the simultaneous control of the transmembrane voltage and recording currents in voltage-clamp mode through multiple channels (Hille 2001).

2.5.2 Recording procedure

To record currents through the *KCNQ5* WT and mutant *KCNQ5* channels in CHO cells were recorded by applying the whole-cell patch clamp technique at room temperature (20°C - 22°C) to transfected cells approximately 24 h post-transfection.

To generate the electrode, borosilicate pipettes were an electrical resistance of 1 - 2 MΩ at the tip. The pulled pipette was then back-filled with an "intracellular" solution containing 140 mM KCl, 2 mM $MgCl_2$, 10 mM EGTA (ethylene glycol-bis (β-aminoethyl ether)-N,N,N′,N′-tetraacetic acid), 10 mM HEPES (4-(2-hydroxyethyl)-1-piperazineethanesulfonic acid), and 5 mM K_2ATP, at pH 7.4 (adjusted with KOH). The medium was changed with an "extracellular" solution of 138 mM NaCl, 5.4 mM KCl, 2 mM $CaCl_2$, 1 mM $MgCl_2$, 10 mM HEPES, and 10 mM glucose, at pH 7.4 (adjusted with KOH). Both solutions had an osmolality in range of 285-295 mOms/kg. A micromanipulator (LN Unit Junior LN, Germany) was used to position the electrode against the cell. Using the Axopatch 200B amplifier controlled by Clampex 10.3 software, the currents were filtered at 2 kHz and digitized at 5 kHz through the Digidata 1320A acquisition system (Molecular Devices, Sunnyvale, CA, USA). The CHO cells were held at a potential of -80 mV, followed by gradual depolarization from -80 mV to +60 mV with an increment of 10 mV for 2 s (Fig.7). To obtain tail currents, a shorter hyperpolarizing

pulse to -120 mV was evoked for 0.5 s.

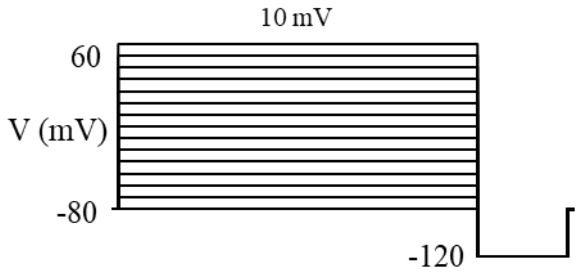

Fig. 7 Voltage step protocols. CHO cells were held at a potential of -80 mV, followed by gradual depolarization from -80 mV to +60 mV with an increment of 10 mV for 2 s. To obtain tail currents, a shorter hyperpolarizing pulse to -120 mV was evoked for 0.5 s.

2.6 Data analysis

The patch-clamp data were copied from the patch-clamp setup computer and analyzed off-line by using Clampfit 10.3 (Axon Instruments) software, Original 6.1 (Original-Lab) software and Excel (Microsoft) on another computer. The activation curve of WT and mutant channels were utilized to plot the normalized the tail (I_{tail}) current peak versus the step potential (V_S). In order to determine the activation curve, the Boltzmann function was fitted to the following data points:

$$I_{tail} = 1/(1+\exp[(V_{1/2}-V_S)/k])$$

where I_{tail} represents the negative peak of the tail current, V_S represents the step voltage, $V_{1/2}$ represents the half-maximal voltage, and k denotes a slope factor.

All data were expressed as the means ± standard error of the mean (SEM). GraphPad Stat-Mate software was used to test the data for a normal distribution of the data. The normally distributed data were analyzed by an unpaired *t*-test and one-way ANOVA with Dunnett's post hoc test to find out the statistical differences between WT and each mutant; the data following a non-normal distribution were analyzed by a Kruskal-Wallis test. Data significance is marked by * $p < 0.05$, ** $p < 0.01$, *** $p < 0.001$, and **** $p < 0.0001$.

3 Results

3.1 Genetics

My colleague, Julian Schubert, conducted a genetic analysis of 238 separate GGE families from the EuroEPINOMICS-CoGIE cohort (May *et al.* 2018) in order to identify novel genes related with the development of GGE in patients. He found two variants (c.1075C>T (p. Arg359Cys, R359C) and c.508G>A (p.Val170Ile, V170I)) in two independent families in a gene that had (at that point) not previously been linked to any disease, namely *KCNQ5*. Recently, this gene has been linked to ID as well as DEE (Lehman *et al.* 2017).

Individuals carrying the p.Arg359Cys variant (family 1) have all been diagnosed with GGE and various epilepsy syndromes including CAE (indicated as I-1 in Fig. 8A), CAE with mildly delayed development (II-2), IGE with mild ID (II-3), and JME with moderate ID (II-5). Interestingly, the developmental delay or ID started prior to seizure onset in two individuals (II-2 and II-3, Fig. 8A), while in individual II-5 (indicated with an arrow in Fig. 8A), the most severely affected patient, the ID was apparent only after seizure onset. The age range of epilepsy onset in family 1 is from 3 to 7 years (Fig. 8A). Notably, individual II-4 is carrying the same variant as the affected family members but has been seizure free until today, indicating reduced penetrance. While seizure freedom was achieved in I-1 (no medication), II-2 and II-3 (under lamotrigine), II-5 only showed a partial response to a combination of lamotrigine, valproic acid and ethosuximide. Generalized irregular 3/s (poly-)spikewave complexes, photoparoxysmal reaction and eyelid myoclonia under photostimulation have been observed in II-2 and II-5 in routine-EEG. Moreover, II-3 presents with generalized spike waves. EEG recordings of I-1 were

not accessible.

Individuals carrying the p.Val170Ile (family 2) variant have all been diagnosed with a form of generalized epilepsy and all affected family members have clear features of JME (indicated in Fig. 8B, I-1, II-1, II-2, II-3). II-1 is the first diagnosed member of family 2, which indicated with an arrow in Fig. 8B. The age range of epilepsy onset in family 2 is from 14 to 21 years (Fig. 8B). I-2 carries the wild type and develops EGTCS approximately once a year not being on antiepileptic treatment. An EEG of I-2 was normal. While seizure freedom was achieved in I-1 (under valproic acid and carbamazepine), II-1 (under valproic acid), and II-3 (under valproic acid), myoclonic seizures worsened in II-2 under lamotrigine. However, after a medication change due to family planning, II-1 showed an exacerbated seizure under lamotrigine and then carbamazepine. Generalized irregular 3-4 Hz (poly-)spike-wave discharge have been observed in I-1, II-1, II-2 and II-3 in routine-EEG.

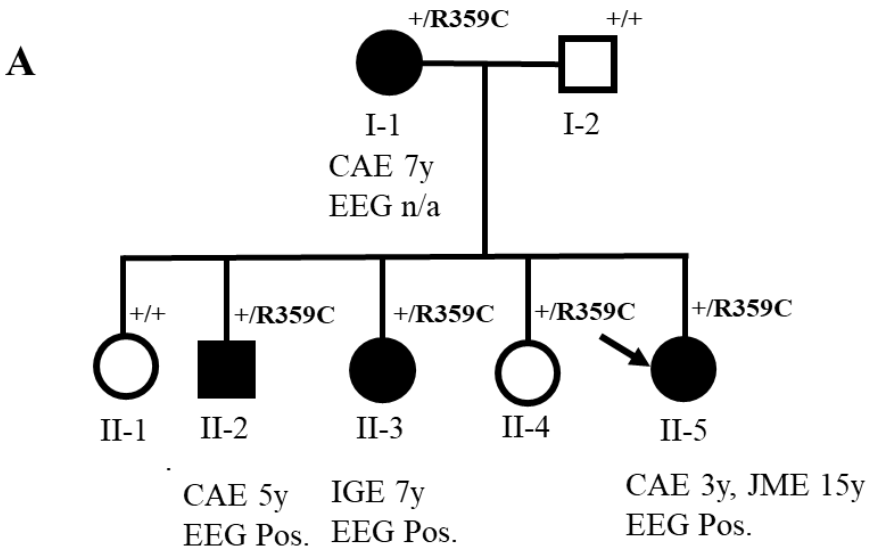

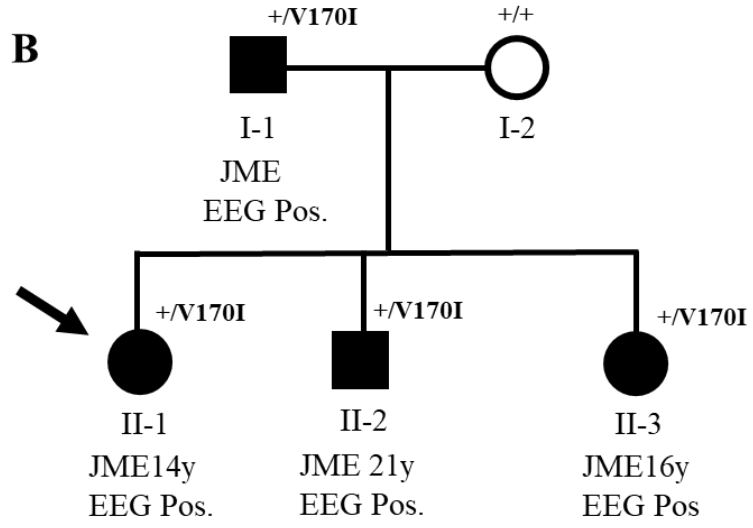

affected female patient
affected male patient
unaffected female patient
unaffected male patient

Fig. 8 Pedigrees of family 1 and family 2. The pedigrees show the phenotype and the genotypes for all family members of **(A)** family 1 (p.Arg359Cys variant and **(B)** family 2 (p.Val170Ile variant). Genotypes are indicated as +/+ for wildtype and +/V170I or +/R359C for heterozygous individuals. The arrow indicates the first individual in the family to be diagnosed. I = first generation, I-1 = first individual of the first generation, II = second generation, II-1 = first individual of the second generation, y = years of age of onset. CAE = childhood absence epilepsy, JME = juvenile myoclonic epilepsy, IGE = idiopathic generalized epilepsy, EEG = electroencephalography, n/a = not available, pos. = positive.

The p.Val170Ile and p.Arg359Cys variants are located in segment S2 and the beginning of the cytoplasmic C-terminus (Fig. 9, p.Val170Ile, orange; p.Arg359Cys, green), respectively. The relevant sections of the *Homo sapiens KCNQ5* protein sequence from UniProt have been aligned with those of *Homo sapiens KCNQ2* and *Homo sapiens KCNQ3* (Table 2) showing that the arginine at position 359 is highly conserved. However, the valine at position 170 is not fully conserved because it is replaced by isoleucine in *KCNQ3* (Table 2).

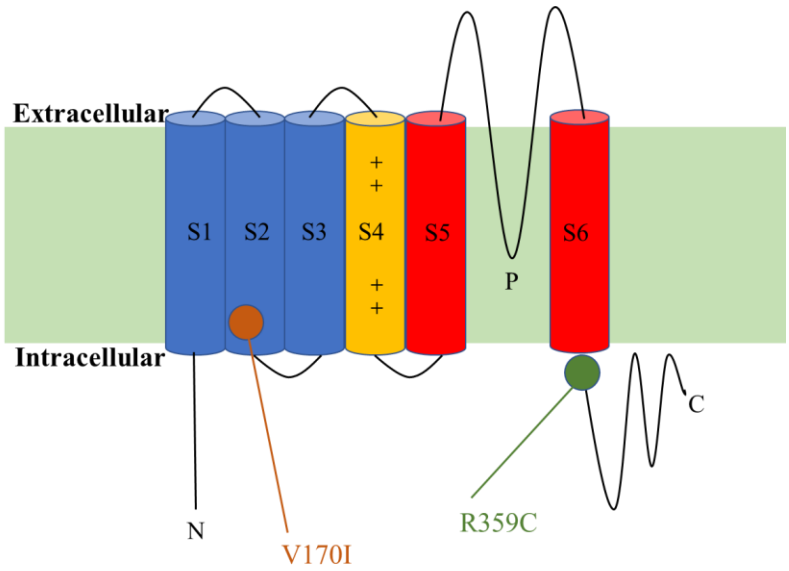

Fig. 9 Structure of the VGPC Kv7.5 subunit. Transmembrane segments of S1-S4 form the voltage sensor domain, and the remaining segments constitute the pore region. The variant p.Val170Ile variant is located in the S2 segments, and the variant p.Arg359Cys variant is located in the proximal cytoplasmic C-terminus. Four of these subunits from the K_V7.5 channel via interaction sites in the C-terminus.

Table 2 Surrounding amino acid sequences of *KCNQ5* variants p.Val170Ile and p.Arg359Cys variants in different *KCNQ* genes in Homo sapiens.

KCNQ* gene in *Homo sapiens	**p.Val170Ile**	**p.Arg359Cys**
KCNQ2	V T I V **V** F G V E	Q E Q H **R** Q K H F
KCNQ3	F A I F **I** F G A E	Q E Q H **R** Q K H F
KCNQ5	V M I V **V** F G L E	Q E Q H **R** Q K H F

3.2 Functional analysis of *KCNQ5* variants

To examine the effects of the *KCNQ5* p.Val170Ile and p.Arg359Cys variants on K_V7.5 channel function, CHO cells were transfected with WT and/or mutant copies of the human *KCNQ5* cDNA. The potassium currents of these exogenous channels in the CHO cell membrane were recorded via a whole-cell patch recording.

3.2.1 Functional analysis of *KCNQ5* p. Arg359Cys

To characterize the effect of the p.Arg359Cys variant on the K_V7.5 channel, CHO cells were transfected with K_V7.5 p.Arg359Cys cDNA (1 µg, n=11), K_V7.5 WT cDNA (1 µg, n=12), and K_V7.5 WT + p.Arg359Cys cDNA in a 1:1 mass ratio (1 µg each, n=13). All cells were recorded via whole-cell patch-clamp to identify potential changes in the electrical properties of the channel induced by the variant. Figure 10 displays exemplary raw current traces of these recorded cells. The results show that, cells transfected with K_V7.5 p.Arg359Cys cDNA or *KCNQ5* WT + p.Arg359Cys cDNA in a mass ratio of 1:1 exhibited a dramatic reduction in current amplitudes compared to those cells only expressing the WT cDNA. Furthermore, the p.Arg359Cys variant showed comparable current amplitudes to those of untransfected CHO cells, which served as controls (n = 7), indicating a complete LOF.

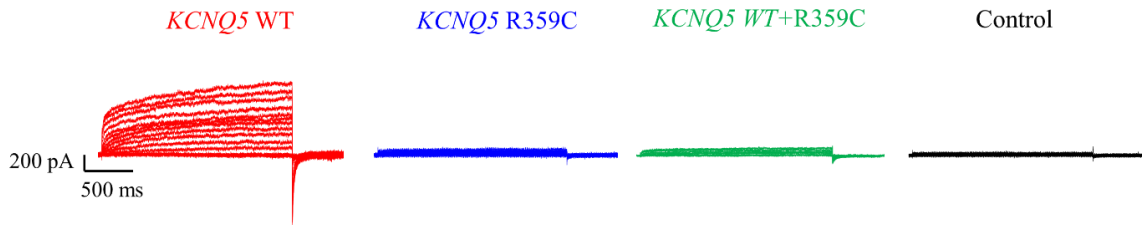

Fig. 10 Representative current traces of non-transfected and *KCNQ5* WT- and/or mutant-transfected cells. Currents observed in CHO cells that were transfected with K_V7.5 WT (1 µg, n=12), K_V7.5 Arg359Cys (1µg, n=11), K_V7.5 WT + p.Arg359Cys (1 µg each, n=13) and untransfected CHO cells (control group, n=7) in response to 10 mV voltage steps from a holding potential of -80 mV to +60 mV. No current was elicited in the control group. Cells transfected with the p.Arg359Cys alone or under WT co-expression show similar currents, which are comparable to the control cells and drastically reduced as compared to the WT.

The row current traces were analyzed for the current density and current density of peak current at +60 mV (Fig. 11). The peak current density is defined as the peak steady state current (in pA) amplitude at +60 mV divided by the whole cell capacitance (in pF). The results show that, homomeric expression of p.Arg359Cys-mutated K_V 7.5 channel subunits led to a dramatically reduced in current amplitudes and peak current densities (Fig. 11). More precisely, the expression of the p.Arg359Cys variant shows such a severe decrease, it is virtually indistinguishable from that in untransfected control cells (peak at 16.7 ± 5.8 pA/pF, n= 11 and 5.6 ± 1.7 pA/pF, n=7, respectively, unpaired *t*-test, $p = 0.0645$, Fig. 11B), only reaching 5.7% (p.Arg359Cys) of current amplitudes recorded in cells transfected with WT channels (peak at 291.6 ± 119.9 pA/pF, n=12, Fig. 11B).

To investigate whether the p.Arg359Cys had a dominant-negative effect on WT subunits, WT and p.Arg359Cys subunits were co-transfected in a 1:1 mass ratio (1 µg each).

Heteromeric expression of WT+p.Arg359Cys led to a minor increase in the current density compared to the homomeric expression of p.Arg359Cys. The peak current density of WT + p.Arg359Cys cells was 48.4 ± 6.6 pA/pF (n=13), which corresponds to only 16.6% as compared to the WT channels. Because the p.Arg359Cys mutant channel exhibited such small current traces (Fig. 10), determining the tail amplitude was not feasible. As a result, an activation curve could not be established. In conclusion, the *KCNQ5* variant p.Arg359Cys causes an almost complete LOF in current density under homomeric expression as well as under co-expression with the WT meaning it has a dominant-negative impact on the WT channels.

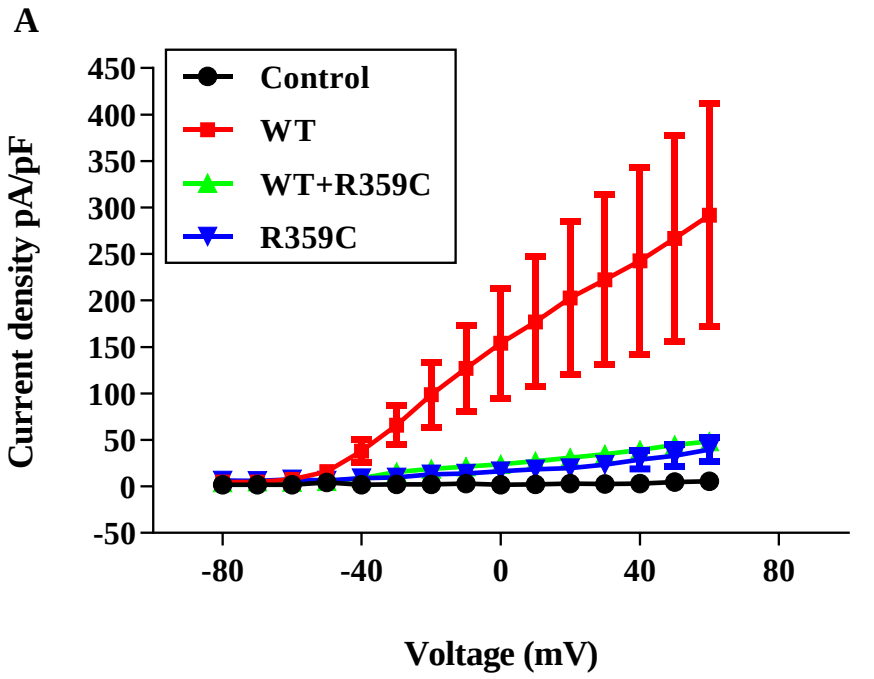
A
Control
WT
WT+R359C
R359C
Current density pA/pF
450
400
350
300
250
200
150
100
50
0
-50
-80
-40
0
40
80
Voltage (mV)

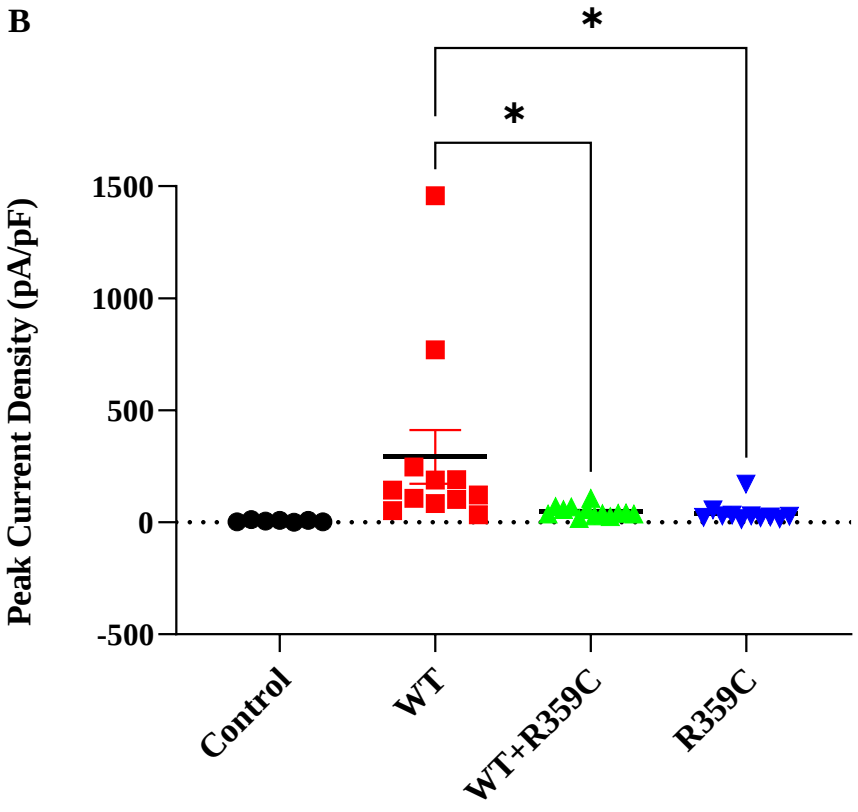
B
*
*
Peak Current Density (pA/pF)
1500
1000
500
0
-500
Control
WT
WT+R359C
R359C

Fig. 11 Peak current density of *KCNQ5* WT- or mutant-transfected and untransfected cells. **(A)** Current density in WT (1 µg, n=12), R359C (1 µg, n=11), WT + p.Arg359Cys (1:1, 1 µg each, n=13) and control (n=7) cells calculated from steady state amplitudes of a 10mV increment step protocol from -80mV to +60mV. **(B)** Peak current density at 60 mV for WT (n=12), p.Arg359Cys359C (n=11), WT + p.Arg359Cys (n=13), and control cells (n=7). All data are shown as mean ± SEM. Data significance is marked by * $p < 0.05$.

3.2.2 Functional analysis of *KCNQ5* p. Val170Ile

To characterize the function of the p.Val170Ile variant in *KCNQ5*, CHO-cells were transfected with K_V7.5 p.Val170Ile cDNA (1 µg, n=8) and compared to cells transfected with WT, K_V7.5 WT cDNA (1 µg, n=12). Judging from the representative current traces, which were derived from CHO cells expressing either K_V7.5 WT or p.Val170Ile mutant channels, the current amplitudes were similar for both expression conditions (Fig. 12).

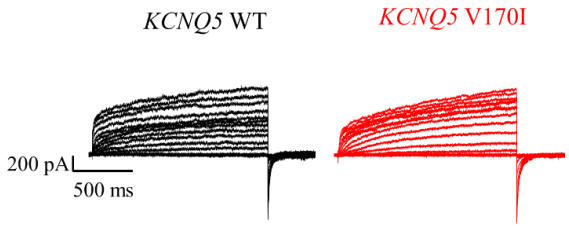

Fig. 12 Representative current traces derived from *KCNQ5* WT and *KCNQ5* p.Val170Ile transfected cells. Representative current traces were derived from CHO cells expressing the K_V7.5 WT channel (n=12) or the K_V7.5 p.Val170Ile (n=8) mutant channels by clamping the transmembrane voltage from a -80 mV holding potential to +60 mV (10 mV increments). The current amplitude of p.Val170Ile is similar to that of the WT.

To analyze the effect of p.Val170Ile on the channel's function, the current density, and the peak current density at +60 mV for homomeric expressed *KCNQ5* WT and the p.Val170Ile expression were analyzed following the descriptions in section 3.2.1 (Fig. 13). CHO cells expressing K_V7.5 p.Val170Ile mutant channels showed lower current density (peak at 156.57 ± 31.53pA/pF, n=8) compared with that of WT (peak at 215.50 ± 61.01 pA/pF, n=12, Fig. 13). However, the peak current amplitude did not show a significant change (p = 0.46, unpaired t-test) between horometrical expressed *KCNQ5* WT and p.Val170Ile subunits.

A

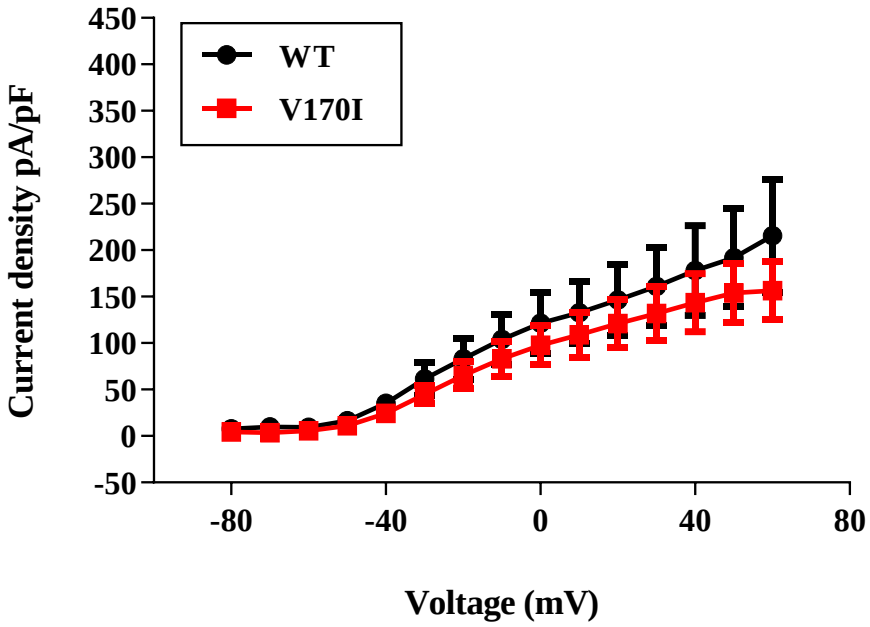
Current density pA/pF
450
400
350
300
250
200
150
100
50
0
-50
WT
V170I
-80
-40
0
40
80
Voltage (mV)

B

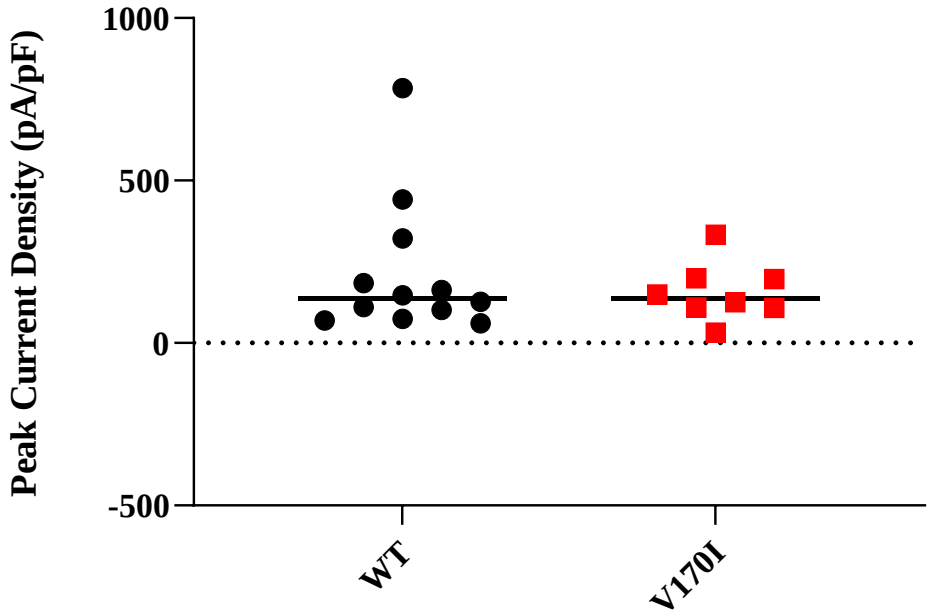
Peak Current Density (pA/pF)
1000
500
0
-500
WT
V170I

Fig. 13 Current density of cells transfected with *KCNQ5* WT and p.Val170Ile. (A) Current density-voltage curve. No significant difference was found in the current density of cells expressing the *KCNQ5* p.Val170Ile mutant channel (n=8) compared to cells expressing the K_V7.5 WT channel (n=12, p = 0.46, unpaired t-test). **(B)** Peak current density at +60 mV of WT (215.50 ± 61.01 pA/pF, n=12) and p.Val170Ile (156.57 ± 31.53 pA/pF, n=8). All data are expressed as the mean ± S.E.M.

The activation curves of the K_V7.5 WT channel (1 µg, n=12) and the K_V7.5 p.Val170Ile mutant channel (1 µg, n=8) were analyzed as well since shifts in the channel activation can also cause a GOF (negative/left shift) or LOF (positive/right shift) while current density remains unaffected. This would mean that the channel opens properly, however, it would do so at more negative (GOF, i.e. facilitated opening) or more positive (LOF, i.e. impaired opening) voltages, respectively. To investigate if this was the case for p.Val170Ile variant, the I/I_{tail}-voltage relationship was established using the negative peak of the tail current, which was induced by a step to -120 mV (to close all channels) at the end of the I-V protocol. The results revealed no apparent shift in the voltage dependence of activation (Fig.14A). The $V_{1/2}$ values, at which half of the channels have opened, of the K_V7.5 WT channel and the K_V7.5 p.Val170Ile mutant channels were -31.63 ± 1.46 mV and -30.03 ± 1.57 mV, respectively (Fig. 14B), and the difference between them is not statistically significant (unpaired t-test, p = 0.47). As this variant does not exhibit any significant differences compared to the WT, it should be considered a benign polymorphism.

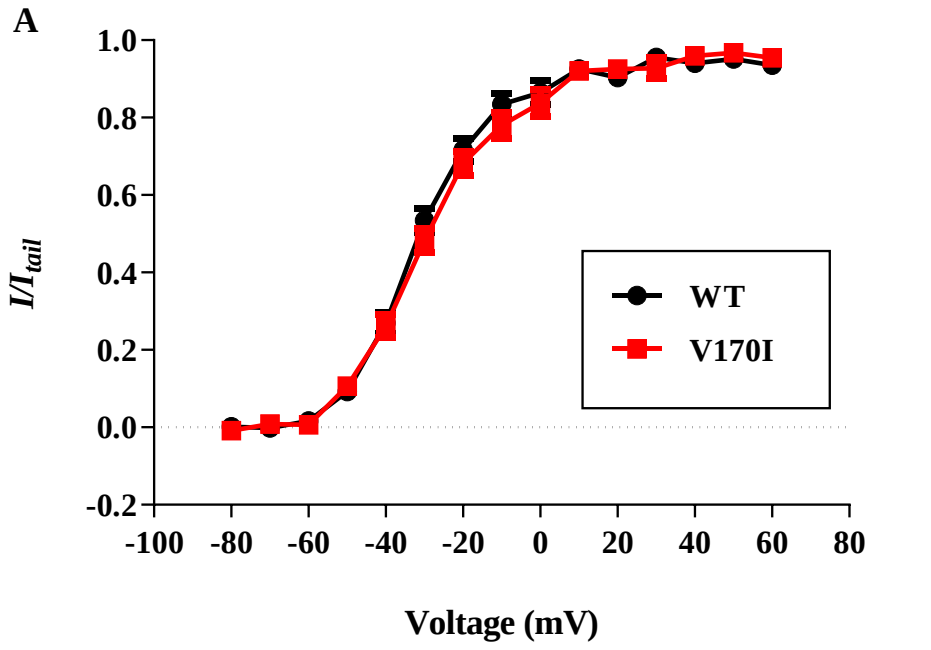
A
1.0
0.8
0.6
0.4
0.2
0.0
-0.2
I/I_tail
-100
-80
-60
-40
-20
0
20
40
60
80
Voltage (mV)
WT
V170I

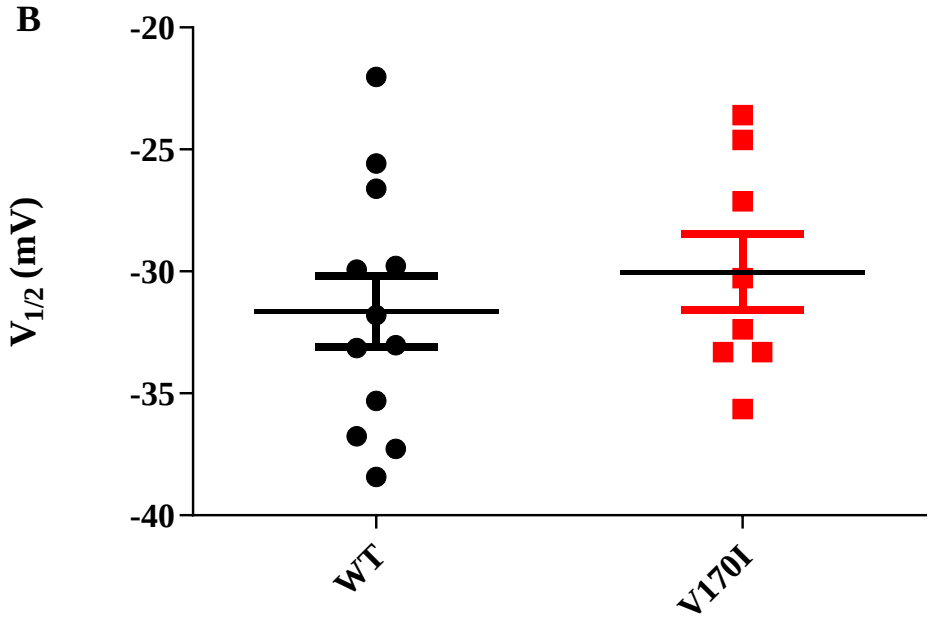
B
-20
-25
-30
-35
-40
V1/2 (mV)
WT
V170I

Fig. 14 Effects of the K_V7.5 p. Val170Ile variant on the activation curve and $V_{1/2}$.

(A) The activation curves of the K_V7.5 WT channel and the K_V7.5 p.Val170Ile mutant channel. The curves were fit using a Boltzmann function. No significant shift in the voltage dependence of activation in the p.Val170Ile variant was observed as compared to the WT. **(B)** Scatter blots of the $V_{1/2}$ values of each cell of the WT (mean -31.63 ± 1.46 mV) and p.Val170Ile (mean -30.03 ± 1.57 mV) channels. The line indicates the mean. No statistically significant difference was observed between the variant and the WT (p = 0.47, unpaired t-test). Data are shown as the mean ± SEM.

In summary, the *KCNQ5* variant p.Arg359Cys exhibits a dominant-negative LOF effect by significantly decreasing the current density even in cells co-expressing the WT cDNA. The p.Val170Ile variant on the other hand has no functional effect and was therefore considered to represent a benign polymorphism.

4 Discussion

The K_V7.5 VGPCs in the CNS and skeletal muscles are encoded by the *KCNQ5* gene. Four *de novo KCNQ5* variants were reported recently to be associated with ID or DEE in 2017 (Lehman *et al.* 2017). The functional analysis of these four *de novo* variants in *KCNQ5* show that three of them result in an LOF by shift in activation, reduced current density or reduced cell surface expression, while the remaining one variant results in a GOF by shifting the activation curve towards more negative potentials. Another study subsequently reported an intragenic duplication of the *KCNQ5* gene in a patient with ID, migraine and absence seizure (Rosti *et al.* 2019). Consequently, researchers have started to focus on variants in the *KCNQ5* gene and study the relationship between K_V7.5 VGPCs and the ethology of various epileptic disorders.

In this study, the functional effect of two *KCNQ5* variants p.Arg359Cys and p.Val170Ile, that had been identified in GGE patients, was investigated.

4.1 The p.Arg359Cys variant induces a loss of function

KCNQ5 variant p.Arg359Cys is located in the cytoplasmic C-terminus. The C-terminus of VGPC K_V7 channel is regarded as a pathophysiological hot-pot for *KCNQ2*-/*KCNQ3*-related epilepsies (Miceli F *et al.* 2010). Rosti and his colleague illustrated haploinsufficiency as a pathomechanism for K_V7.5 variants associated with absence seizures and mild ID in adolescence (Rosti *et al.* 2019). Among the three LOF variants discovered by Lehman and his colleagues (Lehman *et al.* 2017), c.1021C>A (p.Leu341Ile) is located in the C-terminus, which was found to show a dramatic reduced current amplitude, producing a hyperpolarized shift in the voltage dependence on activation. In

my study, the cells with the p.Arg359Cys variant also shows a dramatic drop in the current amplitude, leading to a severe LOF with a decreased current density.

Previously, K_V7-subunit variants in two separate domains, the voltage-sensing domain (S1-S4 segment) and the C-terminus, have been shown to decrease the current (Orhan *et al.* 2014; Maljevic *et al.* 2008; Castaldo *et al.* 2002; Alaimo *et al.* 2009). Variants in the C-terminus of the K_V7 channel impact the function of the C-terminus by controlling intracellularly acting modulators and lowering the current (Soldovieri *et al.* 2014; Cavaretta *et al.* 2014). The C-terminus of *KCNQ* channels is essential in K^+ channel biological processes, participating in channel folding, specific assembly of the subunits, heteromerization, trafficking, and gating (Schwake *et al.* 2003; Haitin and Attali 2008; Li *et al.* 2020). Long C-terminal regions include domains that constitute homomeric or heteromeric subunits and participate in a complex network of numerous molecules, including phosphatidylinositol 4,5-bisphosphate (PI(4,5)P2), calmodulin, syntaxin-1A, and A-kinase-anchoring proteins (AKAPs) (Ambrosino *et al.* 2015). Previous research on PI(4,5)P2 has shown that it has synergistic effects on the S5-S6 region of the K_V7.2-subunit, boosting the voltage sensitivity of the *KCNQ2* channels while upregulating the current amplitude (Zhang *et al.* 2013). As a result, PI(4,5)P2 is essential for maintaining the open state of the K_V7.2, K_V7.4, and K_V7.5 channels (Li *et al.* 2005; Li *et al.* 2020). It is also reported that the pathomechanisms of C-terminal mutations could reduce currents due to impairments of the protein stability (Maljevic *et al.* 2008). Functional interaction between C-termini of the *KCNQ*1 α-subunit and the *KCNE*1 β-subunit was reported to regulate channel deactivation (Zheng *et al.* 2010). The results suggested that both *KCNQ*1-CT and *KCNE*1-CT include an independent interaction domain, which may participate in IKs channel regulation and be subject to some long QT syndrome mutations (Zheng *et al.* 2010). While the N-terminus of *KCNQ* channels is short, the C-termini of

KCNQ channels are longer than other K^+ channels, and these C-termini contain characteristic structural domains (coiled coils, amphipathic α helices containing calmodulin (CaM)-binding motifs and basic amino acid clusters) (Haitin and Attali 2008; Schwake *et al.* 2003). The long C-terminal domain is essential in the normal function and regulation of the $K_V7.2$ channel (Ambrosino *et al.* 2015). According to this study, CaM could bind to two intermittent helices sections in K_V7 channels, known as A helices and B helices, and impact the function of the lengthy intracellular C-terminal domain, on which variations are related with BFNE. $K_V7.2$ channels are thus controlled by altering CaM binding and hence interrupting CaM-induced channel function (Ambrosino *et al.* 2015; Soldovieri *et al.* 2014). My colleague Johanna Krüger repeated and continued and extended studies on the *KCNQ5* variant p.Arg359Cys, finding that the variant critically changes binding to PI(4,5)P2 resulting in the inability of the channel to open. This work has been published so far on bioXriv (Krüger *et al.* 2021) and is under review in a peer-reviewed journal.

The individuals of family 1 display a broad spectrum of different epilepsy syndromes of varying severity, yet they all suffer from GGE. Since all of them carry the same pathogenic variant in *KCNQ5*, but do not share the same phenotype or severity of phenotypic features, it is not possible to establish a genotype-phenotype relationship, more individuals with pathogenic variants in *KCNQ5* would be needed to establish this. The differences in severity of the phenotype in individuals of family 1 might be explained by factors such as compensatory effects, environmental influences, or differences in the remaining genetic background (Miceli F *et al.* 2010).

Therefore, additional studies of the functional effects of variants in *KCNQ5* are warranted. For example, it was reported that variants in *KCNQ* (K_V7) channels affect the surface

expression of VGPCs in the cell membrane (Schwake *et al.* 2000). In future experiments, this possibility could be investigated. Such a drastic dominant negative effect on the M current could potentially result in neuronal hyperactivity and seizures. However, which types of neurons in which brain regions are affected and how this causes generalized seizures must be determined in further experiments. Furthermore, the functional effects of the *KCNQ5* variant p.Arg359Cys in cultured primary neurons should also be examined to observe its influence on neuronal firing, and *in vivo* animal models could also be generated for further studies to address these questions.

4.2 The functional the effect of the p.Val170Ile variant

The *KCNQ5* variant p.Val170Ile is located in the S2 segment. Variants in S1-S2 segment could cause a slight depolarizing shift in voltage dependence of activation of the $K_V7.5$ current, slow down the kinetics of activation and deactivation, and the variants in the S1-S2 region could also be restricted to the subthreshold range (Maljevic *et al.* 2008; Orhan *et al.* 2014). However, in my study the current amplitude of the *KCNQ5* p.Val170Ile transfected CHO cells were similar in size to *KCNQ5* WT transfected CHO cells. The peak current density at +60 mV of the two CHO cell groups, as well as their activation curves, revealed no significant differences. In addition, two benign variants in $K_V7.5$ channels have been reported to share similar electrophysiological recordings to those of the WT (Krüger *et al.* 2021). Therefore, according to the results, the *KCNQ5* variant p.Val170Ile has no functional effect and is considered to be a benign polymorphism not contributing to the phenotype of the affected individuals. We have thus to consider, that not all variants detected in epilepsy patients, and in particularly in GGE, can be laboratory is as pathogenic. Further research preformed in the Epi25 study including our laboratory is working to identify other genetic risk factors in such families, which have been exome-

sequenced.

In summary, we detected two *KCNQ5* variants in two distinct families. Firstly, the LOF variant p.Arg359Cys is associated with GGE and considered to be pathogenic by its dominant-negative effect on WT $K_V7.5$ via decreasing the current density. As a result, the M current is likely diminished in these individuals, leading in a lower action potential threshold and higher excitability of neurons expressing $K_V7.5$ channels, thus increasing seizure vulnerability. Further research is needed to determine the types of neurons and networks involved. Moreover, a benign variant, p.Val170Ile, was investigated in this study, which is considered not to contribute to the phenotype of the affected individuals.

5 Conclusion

5.1 Conclusion

Epilepsy is a common chronic brain disorder of the CNS that affects at least 50 million individuals worldwide and can affect all age groups. It is characterized by recurrent and unpredictable seizures. An increasing number of studies have illustrated that genetic causes could be responsible for idiopathic epilepsy, especially variants in genes encoding ion channels in the cell membrane. Previous studies have already reported that DEEs can be caused by variants in the *KCNQ5* gene. Here, I investigated two *KCNQ5* variants, p.Val170Ile and p.Arg359Cys, from two GGE families. In my experiment, the whole-cell patch-clamp technique was applied to cells transfected with plasmids expressing a mutant or WT *KCNQ5* gene to characterize the functional effects of these two variants. After the analysis of the current traces and the current density of *KCNQ5* p.Val170Ile- and p.Arg359Cys-transfected CHO cells, the p.Arg359Cys variant results in a strong loss of function by reducing the current density even under WT co-expression meaning it has a dominant negative effect. In contrast, the p.Val170Ile variant functions similarly to *KCNQ5* WT and might therefore represent a benign polymorphism that is not related to epilepsy in variant carriers.

5.2 Zusammenfassung

Epilepsie ist eine häufige chronische Hirnstörung, von der weltweit mindestens 50 Millionen Menschen betroffen sind und die in allen Altersgruppen auftreten kann. Sie ist durch wiederkehrende und unvorhersehbare Anfälle gekennzeichnet. Eine zunehmende Anzahl von Studien hat gezeigt, dass genetische Ursachen für die idiopathische Epilepsie

verantwortlich sein könnten, insbesondere Varianten in Genen, die Ionenkanäle in der Zellmembran codieren. Frühere Studien haben bereits berichtet, dass GGE durch Mutationen im *KCNQ5*-Gen verursacht werden können. Hier habe ich zwei *KCNQ5*-Varianten, p.Val170Ile und p.Arg359Cys, aus zwei GGE-Familien untersucht. In meinem Experiment wurde die Ganzzell-Patch-Clamp-Technik auf Zellen angewendet, die mit Plasmiden transfiziert waren, die ein mutiertes oder das WT *KCNQ5*-Gen exprimierten, um die funktionellen Wirkungen dieser beiden Varianten zu charakterisieren. Nach der Analyse der Stromspuren und der Stromdichte von *KCNQ5* p.Val170Ile- und p.Arg359Cys-transfizierten CHO-Zellen führte die p.Arg359Cys-Variant zu einem ausgeprägten LOF und ist damit wahrscheinlich krankheitsverursachend. Die p.Val170Ile-Variant funktioniert hingegen ähnlich wie der *KCNQ5* WT. Sie repräsentiert daher möglichweise einen benignen Polymorphismus und spielt deshalb für die Krankheit bei den Mutationsträgern wahrscheinlich keine Rolle.

6 Reference

Abbott, Geoffrey W, and Steve AN Goldstein. 2002. 'Disease-associated mutations in KCNE potassium channel subunits (MiRPs) reveal promiscuous disruption of multiple currents and conservation of mechanism.' *The FASEB Journal*, 16: 390-400.

Adhikari, S., B. C. Walker, and S. Mittal. 2021. 'Pathogenesis and Management of Brain Tumor-Related Epilepsy.' in W. Debinski (ed.). *Gliomas* (Exon Publications. Copyright: The Authors.: Brisbane (AU)).

Alaimo, A., J. C. Gómez-Posada, P. Aivar, et al. 2009. 'Calmodulin activation limits the rate of KCNQ2 K+ channel exit from the endoplasmic reticulum.' *J Biol Chem*, 284: 20668-75.

Ambrosino, P., A. Alaimo, S. Bartollino, et al. 2015. 'Epilepsy-causing mutations in Kv7.2 C-terminus affect binding and functional modulation by calmodulin.' *Biochim Biophys Acta*, 1852: 1856-66.

Baulac, S., G. Huberfeld, I. Gourfinkel-An, et al. 2001. 'First genetic evidence of GABA(A) receptor dysfunction in epilepsy: a mutation in the gamma2-subunit gene.' *Nat Genet*, 28: 46-8.

Ben-Ari, Y. 2002. 'Excitatory actions of gaba during development: the nature of the nurture.' *Nat Rev Neurosci*, 3: 728-39.

Berkovic, Samuel F., and Ingrid E. Scheffer. 2001. 'Genetics of the Epilepsies.' *Epilepsia*, 42: 16-23.

Biervert, C., B. C. Schroeder, C. Kubisch, et al. 1998. 'A potassium channel mutation in neonatal human epilepsy.' *Science*, 279: 403-6.

Blume, W. T., H. O. Lüders, E. Mizrahi, et al. 2001. 'Glossary of descriptive terminology for ictal semiology: report of the ILAE task force on classification and terminology.' *Epilepsia*, 42: 1212-8.

Brown, D. A. 2008. 'Kv7 (KCNQ) potassium channels that are mutated in human diseases.' *J Physiol*, 586: 1781-3.

Brown, D. A., and P. R. Adams. 1980. 'Muscarinic suppression of a novel voltage-

sensitive K+ current in a vertebrate neurone.' *Nature*, 283: 673-6.

Brown, D. A., and G. M. Passmore. 2009. 'Neural KCNQ (Kv7) channels.' *Br J Pharmacol*, 156: 1185-95.

Brueggemann, Lioubov I, Christopher J Moran, John A Barakat, et al. 2007. 'Vasopressin stimulates action potential firing by protein kinase C-dependent inhibition of KCNQ5 in A7r5 rat aortic smooth muscle cells.' *American Journal of Physiology-Heart and Circulatory Physiology*, 292: H1352-H63.

Castaldo, P., E. M. del Giudice, G. Coppola, et al. 2002. 'Benign familial neonatal convulsions caused by altered gating of KCNQ2/KCNQ3 potassium channels.' *J Neurosci*, 22: Rc199.

Cavaretta, J. P., K. R. Sherer, K. Y. Lee, et al. 2014. 'Polarized axonal surface expression of neuronal KCNQ potassium channels is regulated by calmodulin interaction with KCNQ2 subunit.' *PLoS One*, 9: e103655.

Chen, T., M. Giri, Z. Xia, et al. 2017. 'Genetic and epigenetic mechanisms of epilepsy: a review.' *Neuropsychiatr Dis Treat*, 13: 1841-59.

Claes, L., J. Del-Favero, B. Ceulemans, et al. 2001. 'De novo mutations in the sodium-channel gene SCN1A cause severe myoclonic epilepsy of infancy.' *Am J Hum Genet*, 68: 1327-32.

Cossette, P., L. Liu, K. Brisebois, et al. 2002. 'Mutation of GABRA1 in an autosomal dominant form of juvenile myoclonic epilepsy.' *Nat Genet*, 31: 184-9.

de Lera Ruiz, M., and R. L. Kraus. 2015. 'Voltage-Gated Sodium Channels: Structure, Function, Pharmacology, and Clinical Indications.' *J Med Chem*, 58: 7093-118.

Dorange, Ismet, and Britt-Marie Swahn. 2011. 'Chapter 4 - Recent Progress in the Discovery of Kv7 Modulators.' in John E. Macor (ed.). *Annual Reports in Medicinal Chemistry* (Academic Press).

Dubé, C., A. Vezzani, M. Behrens, et al. 2005. 'Interleukin-1beta contributes to the generation of experimental febrile seizures.' *Ann Neurol*, 57: 152-5.

Duncan, J. S. 1997. 'Idiopathic generalized epilepsies with typical absences.' *J Neurol*, 244: 403-11.

Engel, J., Jr. 2001. 'A proposed diagnostic scheme for people with epileptic seizures and with epilepsy: report of the ILAE Task Force on Classification and Terminology.' *Epilepsia*, 42: 796-803.

Fatt, P., and B. Katz. 1953. 'The electrical properties of crustacean muscle fibres.' *J Physiol*, 120: 171-204.

Fisher, R. S., J. H. Cross, C. D'Souza, et al. 2017a. 'Instruction manual for the ILAE 2017 operational classification of seizure types.' *Epilepsia*, 58: 531-42.

Fisher, R. S., J. H. Cross, J. A. French, et al. 2017b. 'Operational classification of seizure types by the International League Against Epilepsy: Position Paper of the ILAE Commission for Classification and Terminology.' *Epilepsia*, 58: 522-30.

Fisher, Robert S., Walter van Emde Boas, Warren Blume, et al. 2005. 'Epileptic Seizures and Epilepsy: Definitions Proposed by the International League Against Epilepsy (ILAE) and the International Bureau for Epilepsy (IBE).' *Epilepsia*, 46: 470-72.

Foldvary, N., G. Klem, J. Hammel, et al. 2001. 'The localizing value of ictal EEG in focal epilepsy.' *Neurology*, 57: 2022-8.

Füll, Y., G. Seebohm, H. Lerche, et al. 2013. 'A conserved threonine in the S1-S2 loop of KV7.2 and K V7.3 channels regulates voltage-dependent activation.' *Pflugers Arch*, 465: 797-804.

González, C., D. Baez-Nieto, and et al. 2012. 'K(+) channels: function-structural overview.' *Compr Physiol*, 2: 2087-149.

Guerrini, Renzo, Carla Marini, and Carmen Barba. 2019. 'Chapter 1 - Generalized epilepsies.' in Kerry H. Levin and Patrick Chauvel (eds.). *Handbook of Clinical Neurology* (Elsevier).

Gutman, G. A., K. G. Chandy, and et al. 2005. 'International Union of Pharmacology. LIII. Nomenclature and molecular relationships of voltage-gated potassium channels.' *Pharmacol Rev*, 57: 473-508.

Haitin, Y., and B. Attali. 2008. 'The C-terminus of Kv7 channels: a multifunctional module.' *J Physiol*, 586: 1803-10.

Heine, M., A. Ciuraszkiewicz, A. Voigt, et al. 2016. 'Surface dynamics of voltage-gated ion channels.' *Channels (Austin)*, 10: 267-81.

Helbig, I., H. C. Mefford, A. J. Sharp, et al. 2009. '15q13.3 microdeletions increase risk of idiopathic generalized epilepsy.' *Nat Genet*, 41: 160-2.

Hille, B. 1978. 'Ionic channels in excitable membranes. Current problems and biophysical approaches.' *Biophys J*, 22: 283-94.

Hille, B. 2001. 'Ionic Channels of Excitable Membranes (3th ed.).' *(Oxford University Press, Incorporated).*

Hinard, V., A. Britan, J. S. Rougier, et al. 2016. 'ICEPO: the ion channel electrophysiology ontology.' *Database (Oxford)*, 2016.

Hirose, Shinichi. 2014. 'Chapter 3 - Mutant GABAA receptor subunits in genetic (idiopathic) epilepsy.' in Ortrud K. Steinlein (ed.). *Progress in Brain Research* (Elsevier).

Hodgkin, A. L., and A. F. Huxley. 1952. 'A quantitative description of membrane current and its application to conduction and excitation in nerve.' *J Physiol*, 117: 500-44.

Hu, G., F. Niu, B. A. Humburg, et al. 2018. 'Molecular mechanisms of long noncoding RNAs and their role in disease pathogenesis.' *Oncotarget*, 9: 18648-63.

Hunter, J., S. Maljevic, A. Shankar, et al. 2006. 'Subthreshold changes of voltage-dependent activation of the K(V)7.2 channel in neonatal epilepsy.' *Neurobiol Dis*, 24: 194-201.

Janz, D. 1985. 'Epilepsy with impulsive petit mal (juvenile myoclonic epilepsy).' *Acta Neurol Scand*, 72: 449-59.

Janz, D. 1997. 'The idiopathic generalized epilepsies of adolescence with childhood and juvenile age of onset.' *Epilepsia*, 38: 4-11.

Kim, Dorothy M., and Crina M. Nimigean. 2016. 'Voltage-Gated Potassium

Channels: A Structural Examination of Selectivity and Gating.' *Cold Spring Harbor perspectives in biology*, 8: a029231.

Kim, J. B. 2014. 'Channelopathies.' *Korean J Pediatr*, 57: 1-18.

Kim, T. K., and J. H. Eberwine. 2010. 'Mammalian cell transfection: the present and the future.' *Anal Bioanal Chem*, 397: 3173-8.

Kirschstein, T., and R. Köhling. 2016. 'Animal models of tumour-associated epilepsy.' *J Neurosci Methods*, 260: 109-17.

Köhling, R., and J. Wolfart. 2016. 'Potassium Channels in Epilepsy.' *Cold Spring Harb Perspect Med*, 6.

Kors, E. E., A. Melberg, K. R. Vanmolkot, et al. 2004. 'Childhood epilepsy, familial hemiplegic migraine, cerebellar ataxia, and a new CACNA1A mutation.' *Neurology*, 63: 1136-7.

Koutroumanidis, M., G. Bourvari, and S. V. Tan. 2005. 'Idiopathic generalized epilepsies: clinical and electroencephalogram diagnosis and treatment.' *Expert Rev Neurother*, 5: 753-67.

Krüger, Johanna, Julian Schubert, Josua Kegele, et al. 2021. 'Loss-of-function variants in the KCNQ5 gene are associated with genetic generalized epilepsies.' *medRxiv*: 2021.04.20.21255696.

Kuang, Q., P. Purhonen, and et al. 2015. 'Structure of potassium channels.' *Cell Mol Life Sci*, 72: 3677-93.

Kubisch, Christian, Björn C Schroeder, Thomas Friedrich, et al. 1999. 'KCNQ4, a novel potassium channel expressed in sensory outer hair cells, is mutated in dominant deafness.' *Cell*, 96: 437-46.

Kulkarni, S. K., and A. Dhir. 2009. 'Cyclooxygenase in epilepsy: from perception to application.' *Drugs Today (Barc)*, 45: 135-54.

Lehman, A., S. Thouta, G. M. S. Mancini, et al. 2017. 'Loss-of-Function and Gain-of-Function Mutations in KCNQ5 Cause Intellectual Disability or Epileptic Encephalopathy.' *Am J Hum Genet*, 101: 65-74.

Lerche, C., G. Seebohm, C. I. Wagner, et al. 2000. 'Molecular impact of MinK on

the enantiospecific block of I(Ks) by chromanols.' *Br J Pharmacol*, 131: 1503-6.

Li, J., J. Maghera, S. M. Lamothe, et al. 2020. 'Heteromeric Assembly of Truncated Neuronal Kv7 Channels: Implications for Neurologic Disease and Pharmacotherapy.' *Mol Pharmacol*, 98: 192-202.

Li, Y., N. Gamper, D. W. Hilgemann, et al. 2005. 'Regulation of Kv7 (KCNQ) K+ channel open probability by phosphatidylinositol 4,5-bisphosphate.' *J Neurosci*, 25: 9825-35.

Liao, X., M. K. H. Yap, K. H. Leung, et al. 2017. 'Genetic Association Study of KCNQ5 Polymorphisms with High Myopia.' *Biomed Res Int*, 2017: 3024156.

Long, S. B., E. B. Campbell, and R. Mackinnon. 2005. 'Crystal structure of a mammalian voltage-dependent Shaker family K+ channel.' *Science*, 309: 897-903.

Maljevic, S., R. S. Møller, C. A. Reid, et al. 2019. 'Spectrum of GABAA receptor variants in epilepsy.' *Curr Opin Neurol*, 32: 183-90.

Maljevic, S., T. V. Wuttke, and H. Lerche. 2008. 'Nervous system KV7 disorders: breakdown of a subthreshold brake.' *J Physiol*, 586: 1791-801.

Maljevic, S., T. V. Wuttke, G. Seebohm, et al. 2010. 'KV7 channelopathies.' *Pflugers Arch*, 460: 277-88.

May, P., S. Girard, M. Harrer, et al. 2018. 'Rare coding variants in genes encoding GABA(A) receptors in genetic generalised epilepsies: an exome-based case-control study.' *Lancet Neurol*, 17: 699-708.

Meneses, D., A. V. Vega, F. M. Torres-Cruz, et al. 2016. 'KV1 and KV3 Potassium Channels Identified at Presynaptic Terminals of the Corticostriatal Synapses in Rat.' *Neural Plast*, 2016: 8782518.

Miceli F, Soldovieri MV, Joshi N, et al. 2010. 'KCNQ2-Related Disorders. In: Adam MP, Ardinger HH, Pagon RA, et al.' *GeneReviews® [Internet]. Seattle (WA): University of Washington, Seattle*: 1993-2021.

Miceli, F., P. Striano, M. V. Soldovieri, et al. 2015. 'A novel KCNQ3 mutation in

familial epilepsy with focal seizures and intellectual disability.' *Epilepsia*, 56: e15-20.

Milanovska, M., E. Cvetkovska, and S. Panov. 2021. 'Association of rs211037 GABRG2 gene polymorphism with susceptibility to idiopathic generalized epilepsy.' *Med Glas (Zenica)*, 18.

Moeller, Friederike, Ronit M Pressler, and J Helen Cross. 2017. 'Genetic generalized epilepsy.' *Oxford Textbook of Clinical Neurophysiology*: 301.

Nilius, B., and E. Honoré. 2012. 'Sensing pressure with ion channels.' *Trends Neurosci*, 35: 477-86.

Nolan, D., and J. Fink. 2018. 'Genetics of epilepsy.' *Handb Clin Neurol*, 148: 467-91.

Orhan, G., M. Bock, D. Schepers, et al. 2014. 'Dominant-negative effects of KCNQ2 mutations are associated with epileptic encephalopathy.' *Ann Neurol*, 75: 382-94.

Pitkänen, A., K. Lukasiuk, F. E. Dudek, et al. 2015. 'Epileptogenesis.' *Cold Spring Harb Perspect Med*, 5.

Rajakulendran, S., and M. G. Hanna. 2016. 'The Role of Calcium Channels in Epilepsy.' *Cold Spring Harb Perspect Med*, 6: a022723.

Riazi, K., M. A. Galic, and Q. J. Pittman. 2010. 'Contributions of peripheral inflammation to seizure susceptibility: cytokines and brain excitability.' *Epilepsy Res*, 89: 34-42.

Robbins, J. 2001. 'KCNQ potassium channels: physiology, pathophysiology, and pharmacology.' *Pharmacol Ther*, 90: 1-19.

Rosti, G., E. Tassano, S. Bossi, et al. 2019. 'Intragenic duplication of KCNQ5 gene results in aberrant splicing leading to a premature termination codon in a patient with intellectual disability.' *Eur J Med Genet*, 62: 103555.

Sadleir, L. G., K. Farrell, S. Smith, et al. 2006. 'Electroclinical features of absence seizures in childhood absence epilepsy.' *Neurology*, 67: 413-8.

Scheffer, I. E., S. Berkovic, and et al. 2017. 'ILAE classification of the epilepsies:

Position paper of the ILAE Commission for Classification and Terminology.' *Epilepsia*, 58: 512-21.

Scheffer, Ingrid E., and Rima Nabbout. 2019. 'SCN1A-related phenotypes: Epilepsy and beyond.' *Epilepsia*, 60: S17-S24.

Schroeder, B. C., M. Hechenberger, F. Weinreich, et al. 2000. 'KCNQ5, a novel potassium channel broadly expressed in brain, mediates M-type currents.' *J Biol Chem*, 275: 24089-95.

Schwake, M., T. J. Jentsch, and T. Friedrich. 2003. 'A carboxy-terminal domain determines the subunit specificity of KCNQ K+ channel assembly.' *EMBO Rep*, 4: 76-81.

Schwake, M., M. Pusch, T. Kharkovets, et al. 2000. 'Surface expression and single channel properties of KCNQ2/KCNQ3, M-type K+ channels involved in epilepsy.' *J Biol Chem*, 275: 13343-8.

Shah, N. H., and E. Aizenman. 2014. 'Voltage-gated potassium channels at the crossroads of neuronal function, ischemic tolerance, and neurodegeneration.' *Transl Stroke Res*, 5: 38-58.

Soldovieri, M. V., N. Boutry-Kryza, M. Milh, et al. 2014. 'Novel KCNQ2 and KCNQ3 mutations in a large cohort of families with benign neonatal epilepsy: first evidence for an altered channel regulation by syntaxin-1A.' *Hum Mutat*, 35: 356-67.

Stafstrom, C. E., and L. Carmant. 2015. 'Seizures and epilepsy: an overview for neuroscientists.' *Cold Spring Harb Perspect Med*, 5.

Steinlein, O., R. Smigrodzki, J. Lindstrom, et al. 1994. 'Refinement of the localization of the gene for neuronal nicotinic acetylcholine receptor alpha 4 subunit (CHRNA4) to human chromosome 20q13.2-q13.3.' *Genomics*, 22: 493-5.

Suh, B. C., and B. Hille. 2007. 'Regulation of KCNQ channels by manipulation of phosphoinositides.' *J Physiol*, 582: 911-6.

Tjio, J. H., and T. T. Puck. 1958. 'Genetics of somatic mammalian cells. II. Chromosomal constitution of cells in tissue culture.' *J Exp Med*, 108: 259-68.

Vezzani, A., J. French, T. Bartfai, et al. 2011. 'The role of inflammation in epilepsy.' *Nat Rev Neurol*, 7: 31-40.

Villa, Chiara, Marialuisa Lavitrano, and Romina Combi. 2019. 'Long Non-Coding RNAs and Related Molecular Pathways in the Pathogenesis of Epilepsy.' *International journal of molecular sciences*, 20: 4898.

Wallace, R. H., C. Marini, S. Petrou, et al. 2001. 'Mutant GABA(A) receptor gamma2-subunit in childhood absence epilepsy and febrile seizures.' *Nat Genet*, 28: 49-52.

Wang, Q, M_E Curran, I Splawski, et al. 1996. 'Positional cloning of a novel potassium channel gene: KVLQT1 mutations cause cardiac arrhythmias.' *Nature genetics*, 12: 17-23.

Weber, Y. G., S. Biskup, K. L. Helbig, et al. 2017. 'The role of genetic testing in epilepsy diagnosis and management.' *Expert Rev Mol Diagn*, 17: 739-50.

Weber, Y. G., and H. Lerche. 2013. 'Genetics of idiopathic epilepsies.' *Nervenarzt*, 84: 151-6.

Wetsel, W. C. 2011. 'Sensing hot and cold with TRP channels.' *Int J Hyperthermia*, 27: 388-98.

Wuttke, T. V., G. Seebohm, S. Bail, et al. 2005. 'The new anticonvulsant retigabine favors voltage-dependent opening of the Kv7.2 (KCNQ2) channel by binding to its activation gate.' *Mol Pharmacol*, 67: 1009-17.

Xiong, Q., H. Sun, and M. Li. 2007. 'Zinc pyrithione-mediated activation of voltage-gated KCNQ potassium channels rescues epileptogenic mutants.' *Nat Chem Biol*, 3: 287-96.

Zhang, H., L. C. Craciun, T. Mirshahi, et al. 2003. 'PIP(2) activates KCNQ channels, and its hydrolysis underlies receptor-mediated inhibition of M currents.' *Neuron*, 37: 963-75.

Zhang, Q., P. Zhou, Z. Chen, et al. 2013. 'Dynamic PIP2 interactions with voltage sensor elements contribute to KCNQ2 channel gating.' *Proc Natl Acad Sci U S A*, 110: 20093-8.

Zhang, X., D. Yang, and B. A. Hughes. 2011. 'KCNQ5/K(v)7.5 potassium channel

expression and subcellular localization in primate retinal pigment epithelium and neural retina.' *Am J Physiol Cell Physiol*, 301: C1017-26.

Zheng, R., K. Thompson, E. Obeng-Gyimah, et al. 2010. 'Analysis of the interactions between the C-terminal cytoplasmic domains of KCNQ1 and KCNE1 channel subunits.' *Biochem J*, 428: 75-84.

7 Declaration of Contributions to the dissertation

The dissertation work was carried out at the Hertie Institute for Clinical Brain Research (HIH) under the supervision of Prof. Dr. Holger Lerche.

The research was designed by the group of Prof. Dr. Holger Lerche and Dr. Ulrike Hedrich-Klimosch.

After receiving training in laboratory skills from Dr. Ulrike Hedrich-Klimosch, I carried out all experiments and studies.

Statistical analysis was carried out independently with the help of Dr. Ulrike Hedrich-Klimosch.

I confirm that I wrote the manuscript by myself with the supervision of Prof. Dr. Holger Lerche and that any additional source of information has been duly cited.

Signed_____

On_____in Tübingen

8 Acknowledgement

I would like to thank everyone who has helped me in my experiments and thesis writing.

First, I would like to express my gratitude to my supervisor Prof. Dr. Holger Lerche for his constant encouragement and guidance over the past few years. He has so much patience and has given me so much assistance with my experiments, thesis writing, and daily laboratory life.

Second, I want to express my sincere thanks to Xi'an Jiren Hospital, my workplace in China, for supporting me in Germany.

Third, I would like to express my heartfelt gratitude to my second supervisor Dr. Ulrike Hedrich-Klimosch for all her help with experiments and thesis writing. She helped me when I encountered problems with experiments, and she is always patient. When I wrote my thesis, she gave me many good ideas, which was so helpful.

I also want to express my gratitude to Dr. Yuanyuan Liu, PhD student Filip Rosa, Harshad Pa, Johanna Krüger and others in the laboratory. They helped me so much during the past few years in the laboratory and made it possible for me to finish my tasks and my thesis.

Finally, I also want to express my gratitude to my beloved family for supporting me for all these years.